MAKERERE UNIVERSITY

COLLEGE OF AGRICULTURAL AND ENVIRONMENTAL SCIENCES

SCHOOL OF FOOD TECHNOLOGY, NUTRITION AND BIO-ENGINEERING

DEPARTMENT OF AGRICULTURAL AND BIO-SYSTEMS ENGINEERING

DEVELOPMENT OF A SOLAR-POWERED SOIL MOISTURE MONITORING NODE FOR SMART IRRIGATION SYSTEMS

BY

OLEMUKAN ARTHUR

A FINAL YEAR PROJECT REPORT SUBMITTED TO THE DEPARTMENT OF AGRICULTURAL AND BIOSYSTEMS ENGINEERING IN PARTIAL FULFILMENT OF THE REQUIREMENTS FOR THE AWARD OF THE DEGREE OF BACHELOR OF SCIENCE IN WATER AND IRRIGATION ENGINEERING AT MAKERERE UNIVERSITY

MAY 2025

DECLARATION

I **OLEMUKAN ARTHUR,** hereby declare that the contents of this project thesis report are original and have not been submitted for any academic purposes.

Signature: _____ Date: 22/5/2025

OLEMUKAN ARTHUR

2100704913

21/U/04913/PS

This project thesis report has been submitted to my Academic supervisors.

Signature: _____ Date: 22/05/2025

ENG. DR. JOSHUA WANYAMA

Signature: _____ Date: 26/05/2025

DR. ERION BWAMBALE

Digitisation and Self-Archiving Consent Agreement: Theses

Agreement between Makerere University & Students (Authors of Theses / Dissertations / Reports)

1. The author is a student of Makerere University and author of the thesis / dissertation entitled:
DEVELOPMENT OF A SOLAR-POWERED SOIL MOISTURE MONITORING NODE FOR SMART IRRIGATION SYSTEMS

2. The author grants to the University:
   a. The right to deposit the electronic version of the Thesis / Dissertation into Makerere University Institutional Repositories (Mak IR) or (Mak UD); and
   b. The right to store the thesis / dissertation in Mak IR / Mak UD and make it permanently available to the general public via the Internet at no cost to the general public after a grace period (if any is specified).
   Choose one of the two options below:
   c. The Author may opt for immediate open access to the public OPEN ACCESS
   d. Or Restrict access indefinitely or for the specified number of years: .....

3. The author warrants that to the best of the authors knowledge and belief:
   a. The thesis / dissertation is an original work;
   b. The author is the owner of all the intellectual property in the thesis / dissertation;
   or
   c. The Author is entitled to deal with the intellectual property in the thesis / dissertation by publishing it on the Internet
   d. The Author has the right, power and authority to enter into this Agreement and to grant the University the rights contained in this Agreement; and
   e. The University's use of the thesis / dissertation pursuant to this Agreement will not infringe the intellectual property rights of any third party.

4. The Author acknowledges and agrees that the University is not responsible or liable for any breach of the intellectual property rights in the thesis / dissertation, in particular any breach of copyright, as a result of the use of the thesis / dissertation pursuant to this Agreement.

5. The University acknowledges that the rights granted by the Creator in clause 2 of this Agreement, do not cause any transfer or assignment of any proprietary rights in the intellectual property in the article to the University.

Signed by the Author as confirmation that the Author has read and accepted the terms of this Agreement:

Name: OLEMUKAN ARTHUR

College/School: CAES / SFTNB Department: Agricultural and Biosystems Engineering.

(Tick) Type of Degree: (Undergraduate / PGD / Masters / PhD), Reg. No.: _____

Tel No.: 0704421108 E-Mail: olemukanarthur@gmail.com

Signature: Arthur Date: 09/09/2025

Supervisor's endorsement: _____

MakIRs Policy

DEDICATION

I dedicate this report to my loving, caring and supportive mother, Christine Amongin Olemukan, who has continuously supported me financially, spiritually, and morally throughout my education journey. I also extend my gratitude to the rest of my family including my sisters, brothers, uncles, and aunts for their endless prayers for me.

Additionally, I dedicate this project thesis to my friends, whose collaboration and valuable insights greatly contributed to the development of the system design presented here. In the same spirit, I also dedicate this thesis to Mr. Ikabat Joel and Mr. Jotham Mukisa for their invaluable technical guidance and support throughout the completion of this project.

Furthermore, I extend my heartfelt gratitude to the Intellisys Company, under the supervision of Mr. Soddo Paul and Mr. Jjuuko Kenneth, for their invaluable technical support throughout the process of building the sensor node that is documented in this thesis.

Lastly, I dedicate this work to all farmers across the country who are striving to improve agricultural productivity through irrigation, particularly smart irrigation. I hope this work serves as a meaningful contribution and a source of inspiration for your noble efforts.

ACKNOWLEDGEMENT

I would like to thank the Almighty God for the gift of wisdom and the unconditional love he gives me every day. Secondly, I would like to thank the Department of Agricultural and Bio-systems Engineering of Makerere University and the University Administration at large for availing me with this study time to apply the theoretical skills learned in class to real-life problem-solving situations and understanding of the Water and Irrigation Engineering profession at large.

In the same spirit, I extend my heartfelt gratitude to my Academic project supervisors, Eng. Dr. Joshua Wanyama and Dr. Erion Bwambale, for the continuous guidance they've given me throughout this period until I successfully completed this project.

TABLE OF CONTENTS

LIST OF FIGURES

LIST OF TABLES

ABBREVIATIONS

MAAIF – Ministry of Agriculture, Animal Industry and Fisheries

UBOS – Uganda Bureau of Statistics

MUARIK – Makerere University Agricultural Research Institute Kabanyolo

MWE – Ministry of Water and Environment

DABE – Department of Agricultural and Biosystems Engineering

FAO – Food and Agriculture Organization

GDP – Gross Domestic Profit

PVC – polyvinyl chloride

SDGs – Sustainable Development Goals

WUE – Water Use Efficiency

EM – Electromagnetic

TDR – Time Domain Reflectometry

LCD – Liquid Crystal Display

LoRa – Long Range

LoRaWAN – Long Range Wide Area Network

IoT – Internet of Things

Wi-Fi – Wireless Fidelity

CSS - Chirp Spread Spectrum

AI – Artificial Intelligence

WSN – Wireless Sensor Network

GMS – Granular Matrix Sensors

FDR - Frequency Domain Reflectometry

ISM – Industrial, Scientific, and Medical

MHz – megahertz

FSK - frequency shift keying

ADR - Adaptive Data Rate

ET – Evapotranspiration

AC – Alternating Current

DC – Direct Current

ms – milliseconds

MQTT - Message Queuing Telemetry Transport

USB – Universal Serial Bus

RSSI – Received Signal Strength Indicator

SNR – Signal to Noise Ratio

WPAN - Wireless Personal Area Networks

LPWAN – Low Power Wide Area Network

BLE – Bluetooth Low Energy

RFID - Radio Frequency Identification

NB-IoT - NarrowBand IoT

GSM - Global Systems for Mobile Communication

EC-GSM - Extended Coverage Global Systems for Mobile Communication

dBm – decibel milliwatt

BMS – Battery Management System

EUI – Extended Unique Identifier

OTAA – Over-The-Air-Activation

DEVEUI – Device Extended Unique Identifier

APPEUI – Application Extended Unique Identifier

CAEC – Continuing Agricultural Education Center

JSON – JavaScript Object Notation

IoT – Internet of Things

ABSTRACT

This project presents the development of a solar-powered, LoRa-based soil moisture monitoring sensor node aimed at improving irrigation scheduling in smart agricultural systems. The system addresses challenges such as unreliable grid power, limited internet connectivity, and short-range communication in traditional IoT-based irrigation technologies. The sensor node integrates an Irrometer Model 200SS Watermark tensiometric sensor, Arduino Uno microcontroller, LoRa SX1276 transceiver, and a solar-powered energy system. Deployed at the MUARIK irrigation demonstration site, it successfully monitored real-time soil water tension and transmitted data to a LoRa gateway without internet dependency. The watermark sensor was calibrated and validated against the gravimetric method, producing two linear equations ($R^2 > 0.96$), while validation using a two-tailed t-test gave a p-value of 0.673, confirming correlation between the sensor and gravimetric results. Real-time soil water tension was categorized by a Python-based decision algorithm into wet, moist, and dry. When soil reached the dry threshold (≥60 kPa, 17.521 g/g), a downlink message opened a Strega smart valve for irrigation, which continued until tension dropped to ≤9 kPa (32.581 g/g), automatically closing the valve and preventing over-irrigation. The process was autonomous with a 1-minute update cycle. Field tests showed best performance when the gateway had clear line of sight, with higher RSSI and SNR at the farm shelter compared to CAEC. Overall, the system reduced manual labour, improved water use efficiency, and proved viable for off-grid deployment. Recommendations include placing the gateway in clear line of sight, deploying more nodes for zoned irrigation, and integrating a mobile dashboard for real-time monitoring.

CHAPTER ONE: INTRODUCTION

1.1 Background of the Study

Agriculture is considered to be the backbone of many developing country economies which is a similar trend in Uganda. The Ministry of Agriculture, Animal Industry, and Fisheries (MAAIF) associated agriculture with employing 73% of the population, while contributing 23% to the gross domestic profit (GDP) of the nation (Bamwesigye et al., 2020). However, the agricultural sector faces very many significant challenges which are majorly related to the climate variability such as the droughts, erratic rainfall and rising temperatures. These have increasingly affected the food security and agricultural productivity.

Policy makers all around the world have stressed the importance of irrigation in enhancing food security amidst the climate variability (Wanyama et al., 2017). Climate variability has increasingly led to the adoption of irrigation as a way of ensuring sustainable food production in order to meet the food needs of the rapidly growing population. This population currently stands at 45.9 million as per the population census which was carried in June 2024 by UBOS (UBOS, 2024). Globally, the population stands at 7.951 billion and growing at an annual rate of 0.87%. It is projected to rise from the current 8 billion to approximately 9.7 billion by 2050 (United Nations, 2024).

In Uganda, initiatives such as the World Bank-supported micro-scale irrigation program which is administered by the Ministry of Agriculture, Animal Industry and Fisheries (MAAIF) aim to promote the sustainable agricultural practices by providing the smallholder farmers with subsidized irrigation equipment and training. Additionally, the Food and Agricultural Organization (FAO) is highly focusing its resources on irrigation development projects particularly precision irrigation in order to provide solutions to the overarching problems of climate variability in agriculture (Jara-Rojas et al., 2018).

Smart irrigation integrates intelligent decision-making techniques to optimize the water usage by applying it at the right time and amount which improves the agricultural productivity and reduces on the environmental impacts (Vallejo-g et al., 2023). Additionally, it integrates advanced technologies such as sensors and information systems and has emerged as one of the key solutions to the challenges posed by climate variability. Precision irrigation in particular plays a pivotal role

by ensuring that the crops receive water at the right time and in the right amounts (Jara-Rojas et al., 2018). This approach greatly improves the water use efficiency (WUE), contributing to the sustainable agriculture and aligning with the United Nations' Sustainable Development target 6.4 which emphasis on improving the water use efficiency (Sui, 2018).

In order to cope up with the gradual increase in the demand of food, technological advancements such as Internet of Things (IoT) and Wireless Sensor Networks (WSNs) have facilitated the development of smart irrigation systems. Some of these systems use electromagnetic (EM) sensors to measure soil moisture levels and providing real-time data to optimize the irrigation schedules according to Datta et al., (2018). The most commonly used IoT technologies include; low-power Wireless Fidelity (Wi-Fi), Bluetooth Low Energy (BLE), DASH7 Alliance Protocol (D7A) among others.

While the IoT-based smart farming technologies show great potential for improving the agricultural productivity and optimizing the water use, the adoption of their sensor nodes faces very many significant obstacles such as frequent power outages, limited range of coverage and limited internet connectivity in particular areas. To address these gaps, reliable technologies like LoRa have been adopted due to their suitability for low power consumption, long-range coverage, and ease of deployment (Ting & Chan, (2024).

As part of efforts to enhance irrigation scheduling, Makerere University's Department of Agricultural and Biosystems Engineering (DABE) partnered with Agriscope, a Swiss-based company specializing in agricultural sensor technologies. This collaboration led to the deployment of a LoRa-based smart irrigation system at the MUARIK. The system utilizes Irrometer Model 200SS Watermark sensors to monitor real-time soil moisture tension. The collected data packets are transmitted wirelessly to Agriscope servers located in France, where they are logged and accessed via custom code written to retrieve the data.

When dry soil conditions are detected, the system automatically sends a downlink message from the gateway to open Strega smart valves, initiating irrigation. Irrigation continues until the soil moisture reaches field capacity, at which point another downlink message is sent to close the valves, effectively ending the irrigation cycle. While this setup has demonstrated the ability to automate irrigation, a major limitation remains that the data is not locally accessible. Users must notify the third-party service in France to request the data which introduces a time lag that delays

decision-making. Additionally, accessing the data requires an annual subscription, which increases the operational cost due to third-party involvement.

In pursuit of a more localized and self-sufficient smart irrigation system, Mr. Ikabat Joel, a DABE alumnus, successfully configured the Strega smart valves to communicate directly with the LoRa gateway. The remaining step was the development of a locally built soil moisture sensor node. Once completed, this node would transmit real-time data from the field directly to the gateway. This will enable timely and accurate irrigation decisions without external dependencies, allowing the gateway to send appropriate downlink commands to the Strega valves such as to irrigate when needed or remain closed when soil moisture is sufficient.

This study aimed to develop a solar-powered soil moisture monitoring sensor node integrated with LoRa technology. The sensor node will harness renewable energy to address challenges such as frequent power outages, limited communication range, and reliance on internet connectivity. It will measure real-time soil moisture tension values and wirelessly transmit the data to a LoRa gateway. This approach will facilitate the creation of informed irrigation schedules directly on the farm, enhancing irrigation efficiency and sustainability by ensuring that the data required for scheduling is readily and locally available.

1.2 Problem Statement

Most of the current smart irrigation systems are incorporated with advanced communication technologies such as the use of the wireless sensor networks which are a form of the Internet of Things (IoT) technology used to monitor and manage irrigation processes. These systems typically rely on sensor nodes which are installed in agricultural fields to track the real time soil moisture conditions.

Despite the fact that the IoT-based solutions provide valuable insights for irrigation scheduling, they also present several limitations. Some of these key challenges include, frequent power outages due to dependence on grid electricity, limited coverage range, high power consumption, and the requirement for constant internet connectivity. These constraints hinder the reliable transmission of soil moisture data, leading to inaccurate or uninformed irrigation decisions. Consequently, this

results in either over-irrigation or under-irrigation, both of which negatively affect water use efficiency and crop productivity.

This study proposes a solution to these challenges by designing and developing a solar-powered, LoRa-based soil moisture monitoring sensor node for real-time irrigation scheduling. The system integrates LoRa (Long Range) technology, which is known for its low power consumption, long-range communication capabilities, and independence from internet-based infrastructure. Powered by solar energy, the sensor node eliminates reliance on unreliable or unavailable grid power, making it suitable for off-grid agricultural environments.

1.3 Objectives of the Study

1.3.1 Main Objective

The main objective of this study is to develop a solar-powered, LoRa-based soil moisture monitoring sensor node for real-time soil moisture monitoring to enhance irrigation scheduling.

1.3.2 Specific Objectives

The specific objectives of this study are:

i. To design and construct a solar-powered, LoRa-based soil moisture monitoring sensor node.
ii. To program and configure the sensor node for accurate real-time soil moisture monitoring and seamless communication with the existent smart LoRa-based irrigation system.
iii. To evaluate the performance of the sensor node in enhancing irrigation scheduling.

1.4 Research Questions

i. What are the design and technical specifications required to develop a solar-powered soil moisture sensor node integrated with LoRa technology?
ii. How can the sensor node be programmed and configured to ensure accurate real-time soil moisture monitoring and seamless communication with the existent LoRa-based smart irrigation system?

iii. How effectively does the sensor node enhance irrigation scheduling in the smart irrigation system?

1.5 Significance of the Study

Globally, approximately 70% of freshwater resources are used to irrigate 25% of the world's croplands which supply 45% of the global food needs (Koech & Langat, 2018). These statistics highlight the increasing need of optimizing water use to sustain the agricultural productivity. In this context, smart irrigation systems that are integrated with drip irrigation provide a solution by improving water use efficiency, enhancing crop productivity and conserving scarce water resources. This approach aligns with the Sustainable Development Target 6.4 which aims to improve the water use efficiency across all sectors by 2030.

In Uganda, where agriculture remains the backbone of the economy, smart irrigation faces significant challenges such as frequent power outages and limited internet connectivity (Bezerra et al., 2019). Addressing these barriers requires innovative solutions such as leveraging LoRa radio technology which is famously known for its low power consumption, long range coverage and easy deployment. LoRa radio technology is ideal smart farming applications, particularly in remote settings where resilient communication is needed (Ting & Chan, 2024b).

This study is significant as it seeks to develop a solar-powered moisture sensor node using LoRa technology to address these common challenges. The solution is designed to overcome limitations in communication range, compatibility with existing LoRa irrigation systems, and reliance on unstable power sources. Furthermore, the study explores the potential of integrating LoRaWAN technology to establish a scalable, robust smart irrigation network capable of real-time soil moisture monitoring (Haxhibeqiri et al., 2018).

By enabling seamless communication between the sensor node and a LoRa gateway, the system will support the generation of timely and accurate irrigation schedules. The outcomes of this research are expected to enhance water use efficiency, promote sustainable agriculture, and offer a scalable model for smart irrigation in resource-constrained settings

1.6 Scope and Limitations of the Study

1.6.1 Scope

This project focuses on developing a solar-powered, LoRa-based soil monitoring sensor node that will track the real-time soil moisture condition and reliably transmit the data packets over a Long-Range Wireless Area Network (LoRaWAN) for proper generation and adjustment of irrigation schedules. The system comprises of a sensor node and the control unit. The sensor node comprises of one Irrometer Model 200SS Watermark sensor housed in a PVC pipe, an Arduino uno microcontroller, a 20 by 4 LCD display screen, an Ebyte SX1276 LoRa sender module, three rechargeable lithium-ion batteries, a solar charge controller and a solar panel. Secondly, the control unit comprises of a LoRa gateway built using a Raspberry Pi 4, SX 1302 Hal receiver LoRa module and programmed using the ChirpStack software. Data packets from the field are transmitted wirelessly over the LoRaWAN to the control unit (gateway) where the irrigation schedules are generated or adjusted accordingly. When dry conditions are detected, the system automatically sends a downlink command to the Strega smart valve to initiate irrigation, which continues until the soil moisture is restored, after which the valve is instructed to close. The system was deployed at the MUARIK, DABE irrigation demonstration site for site testing and collection of data which was used by farmers to make informed irrigation decisions based on reliable data.

1.6.2 Limitations

Testing of the solar-powered, LoRa-based soil moisture monitoring sensor node was limited to only the MUARIK, DABE irrigation demonstration site and was not extended to other farm settings. Additionally, the high cost of components required to build the sensor node limited the study from being tested and executed on a large scale.

1.7 Conceptual Framework

The conceptual framework of this study is illustrated in Figure *1.1* below. It clearly defines the independent, mediator, moderate and dependent variables used in the study. The independent variables include the sensor design parameters, solar power system, communication network and the deployments conditions. At the center of the framework are the mediator variables which are

influenced by the moderator variables. On the far right of the framework are the independent variables that represent the outcomes from the study.

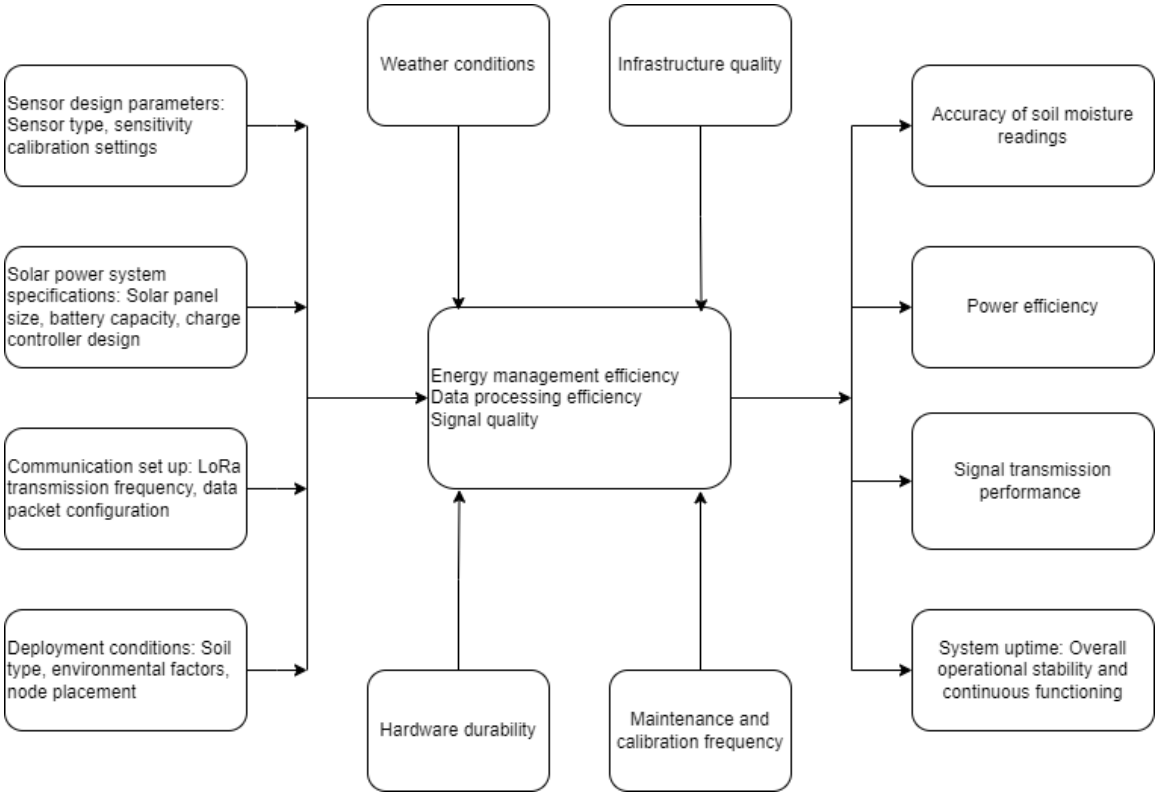

Figure 1.1: Conceptual Framework

CHAPTER TWO: LITERATURE REVIEW

This chapter covers the basic knowledge about smart irrigation systems, especially the application of IoT in automating the smart irrigation systems.

2.1 Traditional irrigation systems

Irrigation is the artificial application of water to the soil with the purpose of boosting crop production. Water can either be pumped or delivered through pipelines, canals, or natural streams from rivers, reservoirs, lakes, or aquifers by gravity. Irrigation is the backbone of agriculture, and it has very many methods including drip, sprinkler, furrow, basin and strip irrigation systems. Among these, drip and sprinkler irrigation systems are categorized as pressurized irrigation systems while furrow, border and basin irrigation systems are classified as surface irrigation systems (Pradesh, 2018).

2.1.1 Surface irrigation systems

Surface irrigation systems are widely used due to their simplicity and cost-effectiveness. These methods distribute water across the soil surface to irrigate crops without requiring advanced technology, making them accessible to farmers. However, surface irrigation generally demands more physical effort compared to other irrigation methods (Pradesh, 2018).

The benefits of surface irrigation are notable. Minimal capital investment is required for construction at the farm level, making it affordable for farmers. The critical structural components are located at the field's edges, simplifying operation and maintenance. Additionally, these systems rely on gravity as their energy source, removing the need for external power, and are less affected by climate and water quality variations. Their adaptability and ease of management make surface irrigation systems a practical choice for diverse agricultural needs.

2.1.2 Sprinkler irrigation systems

Sprinkler irrigation systems mimic natural rainfall by spraying water into the air, which then falls onto the ground for effective irrigation. This system uses nozzles to enhance water pressure, ensuring even water distribution. Uniform irrigation is achieved by selecting the right nozzle sizes, maintaining proper sprinkler spacing (typically 65% of the wetted diameter), and operating at the correct pressure. This method is especially effective for areas with uneven terrain or shallow soils (Darko et al., 2017; Pradesh, 2018). One of the key advantages of sprinkler irrigation is its ease of

operation and lower labour requirements. It is adaptable to all soil types except heavy soils and can help protect crops from frost and high temperatures. Additionally, it eliminates drainage problems, making it a versatile choice for farmers in various conditions (Pradesh, 2018).

2.1.3 Drip irrigation systems

Drip irrigation systems deliver water directly to the root zone of crops or below the soil surface at a low discharge rate using emitters or drippers. This method maintains consistent soil moisture levels by supplying water continuously, drop by drop, creating a wet bulb in the root zone from which plants absorb water. The wet bulb's size depends on the emitter's discharge rate and soil properties such as hydraulic conductivity and texture. Drip irrigation is considered the most efficient irrigation method as it optimizes water use and minimizes wastage (Jarwar et al., 2019).

The advantages of drip irrigation are significant. By delivering water directly to the roots, it conserves water and saves energy as it operates at lower pressures. It also facilitates efficient application of fertilizers and chemicals, reducing waste while improving nutrient delivery to plants. Furthermore, this method requires less manual labour, making it cost-effective, and is suitable for use in hilly terrains. Drip irrigation enhances crop yields and improves the quality of agricultural produce, making it an indispensable tool for modern farming (Jarwar et al., 2019; Pradesh, 2018)

2.2 Smart irrigation systems

Smart irrigation systems are systems that involve the integration of sensors, controllers and communication technologies into irrigation systems to optimize water use and crop yields. They are continuously emerging as the new advanced disciplines that use data-intensive methods to increase agricultural productivity while increasing the environmental sustainability (Obaideen et al., 2022). Modern irrigation operations generate data from a variety of sensors which greatly lead to a better understanding of both operation environment and the operation activities. (Tantalaki et al., 2019). This approach leads to more effective and efficient decision-making.

Smart irrigation systems improve the WUE and are an emerging method that automates irrigation while conserving water. This technique adjusts irrigation based on the real-time soil and weather conditions which in turn enable the farmers to meet their needs using a new approach that helps

conserve water during the irrigation process (Obaideen et al., 2022). **Figure *2.1*** shows the smart irrigation system layout which comprises of data acquisition (sensor), irrigation control, wireless communication, data processing and fault detection.

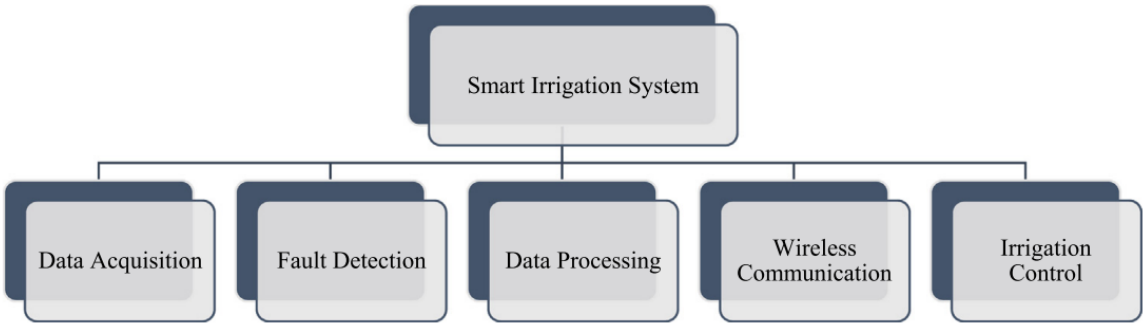

Figure 2.1: Layout of a smart irrigation system (Sourced from: Obaideen et al., 2022)

IoT, smartphone applications, and sensors enable the farmers to easily monitor the conditions of their fields such as detecting soil temperature, water requirements, weather patterns among others. IoT is an extension of the internet which connects two or more device which are capable of communicating with electronic systems and linking them to the internet. This extension greatly impacts these devices by simplifying their use and operation (Velmurugan et al., 2020). In this context, IoT is integrated into the automation of agricultural practices, such as connecting soil moisture sensor nodes to control units, enhancing productivity and efficiency across farming operations such as real-time soil moisture monitoring. Furthermore, the use of sensors is also important to the farmers because they enable them understand their crops better and help to reduce the environmental impacts and conserve water resources (Obaideen et al., 2022). Despite the adoption of smart irrigation systems, most of them lack the integration with renewable energy sources which limits their adoption in rural and off-grid areas.

2.3 Irrigation scheduling

Irrigation scheduling is the planning of the timing and depth of future irrigation. Its primary goal is to know when and how much water to apply in the field. The most common irrigation criteria used to determine the need for irrigation are the soil moisture content and soil moisture tension. The common irrigation scheduling methods are: Feel and appearance, Gravimetric method,

Weather-based irrigation scheduling, sensor based-irrigation scheduling, IoT sensor technology and Smartphone APP (Gu et al., 2020).

2.3.1 Gravimetric method

This method involves collecting samples and measuring their actual soil moisture content. It is highly accurate and involves the weighing of a soil sample of a known volume, drying it in an oven at 105 ºC and then reweighing it to determine the mass of water lost by drying. This method enables the calculation of gravimetric water content (g/g) and soil bulk density (g/cm^3). Multiplying the gravimetric water content by the soil bulk density allows for calculating the volumetric water content (cm^3/cm^3). The equation for volumetric water content is described in Equation *2.1*. The soil sample collection method is very accurate but it requires intense labour, time and soil disturbance. Therefore, continuous soil moisture monitoring through sample collection in the field can be difficult and limited.

$$\theta v = \frac{\theta g * \rho soil}{\rho water} = \frac{\left(\left(\frac{Mwater - Mdry}{Mdry}\right) * \left(\frac{Mdry}{Vsoil}\right)\right)}{\rho water}$$

Equation 2.1

Where;

$\theta v =$ Volumetric water content (cm^3/cm^3)

$\theta g =$ Gravimetric water content (g/g)

2.3.2 Plant-based irrigation scheduling method

According to Jones, (2004), plant-based irrigation scheduling focuses on monitoring plant responses to water deficits rather than relying completely on the soil moisture or water balance methods. This method offers a direct measure of the plant water stress which can be highly sensitive to the changing water conditions (Gu et al., 2020). The main methods include:

2.3.2.1 Direct Measurements of Plant Water Stress

This comprises of leaf water potential, stem water potential and the relative water content.

2.3.2.2 Plant Physiological responses

These responses include the stomatal conductance, growth rate and sap flow.

2.3.2.3 Advanced Techniques

The advanced techniques include infrared thermography and cavitation detection (Vories & Sudduth, 2021).

2.3.3 Soil moisture-based irrigation scheduling

According to Gu et al., (2020), this method of irrigation scheduling involves the use of sensors to monitor soil water content and trigger irrigation when moisture levels drop below predefined thresholds. These thresholds are typically determined through field experiments or derived from crop and soil-specific studies. The system ensures water is applied precisely, either to refill the soil to its field capacity or to a slightly lower level to avoid over-irrigation and deep percolation. Various sensors, such as capacitance probes or tensiometers, measure soil moisture or tension, while more advanced systems integrate dynamic thresholds that adjust for crop type, growth stage, and soil properties.

This method offers several advantages, including improved water use efficiency, better crop yields, and the ability to adapt to spatial and temporal variations within fields. It is particularly effective when combined with wireless networks or decision-support systems for field-scale management. However, challenges such as sensor accuracy, calibration, and threshold variability must be addressed. Innovations like IoT-enabled controllers and machine learning models can enhance the effectiveness of this approach by automating irrigation and providing real-time data for precise decision-making. Soil moisture-based scheduling is an integral component of modern irrigation strategies, supporting sustainable water management and optimal agricultural productivity (Gu et al., 2020). This project will focus on the soil moisture-based method of irrigation scheduling.

2.4 Soil moisture monitoring

According to Rasheed et al., (2022), soil moisture is an important component on a small agriculture scale as well as large agriculture scale modeling. Crops depend on the root level of moisture present in the soil. Having knowledge about the amount of moisture in the soil is essential for all the farmers because it allows them to assess the field conditions and take appropriate actions. The soil moisture levels indicate the amount of water present in the soil and can be expressed in terms of mass or volume.

When based on mass, soil water content is represented by the gravimetric soil moisture content, denoted as θg shown in Equation *2.2*:

$$\theta g = \frac{Mwater}{Msoil}$$

Equation 2.2

Where $Mwater$ is the mass of the water in the soil, and $Msoil$ is the mass of the dry soil present in the field.

The volumetric soil moisture content of a soil θv, is defined by Equation *2.3*:

$$\theta v = \frac{Vwater}{Vsample}$$

Equation 2.3

Where $Vwater$ is the volume of water content in the soil and $Vsample$ is the total volume of soil sample obtained from the field.

Soil moisture is a very crucial parameter in the growth of plants and therefore, proper monitoring of soil moisture is needed in order to maintain an optimal irrigation schedule (Obaideen et al., 2022). Effective and efficient monitoring systems play a very crucial role in the growth of plants and their development. These systems are essential for creating an irrigation control system that maximizes food production while minimizing water loss (Garc et al., 2020). Precision irrigation involves the gathering of data to accurately represent the real-time conditions of the plants, soil, and weather in irrigation areas while utilizing IoT and WSNs. IoT has enabled the development of cost-effective technology to improve irrigation monitoring and control. Furthermore, WSNs support the real-time monitoring in precision agriculture by deploying a network of wireless sensor nodes that sense, process, and transmit data on various parameters (Sciences, 2024).

Soil moisture sensor-based systems can primarily be categorized into two type which are the suspended cycle irrigation system and the water-on-demand irrigation system. The suspended cycle system operates on a traditional timer which is controlled with preset schedules for irrigating which comprises of the start and end times. These systems automatically stop the next scheduled irrigation when the moisture in the soil is sufficient enough. On the other hand, the water-on-demand system does not require programming or set irrigation durations. It involves the farmer

setting a moisture threshold, and irrigation is triggered whenever the soil moisture falls below this level (Goap et al., 2018).

There are several techniques that are used to indirectly measure the soil moisture content and some are illustrated in Figure *2.2*. All the methods for measuring soil moisture have their own advantages and disadvantages which should be taken into account depending on the project's requirements and demand (Sharma et al., 2018).

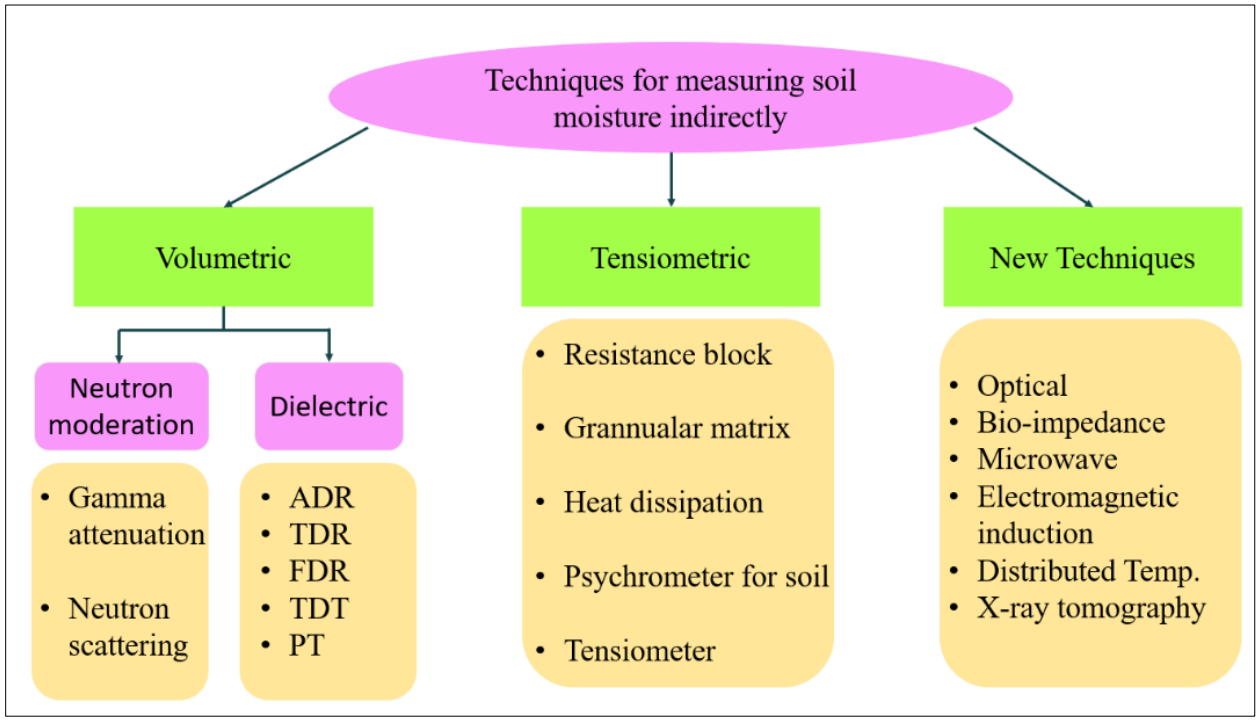

Figure 2.2: Techniques of measuring soil moisture indirectly (Source: Vera et al., 2021)

2.4.1 Volumetric techniques

These techniques indirectly determine the soil moisture content as a percentage of the soil volume. These techniques are mostly used for real-time irrigation management decisions (Vera et al., 2021). These techniques employ a variety of principles which are broadly used to classify them in to Dielectric sensors and Neutron moderation.

2.4.1.1 Dielectric sensors

These sensors operate by determining the soil's dielectric constant. It measures a nonconducting materials' ability to transmit electromagnetic waves or pulses. Because the dielectric constant of dry soil is lower than that of water, even small changes in the quantity of soil will have a significant impact on the electromagnetic properties of the soil water. An alternating electric field is generated in the surrounding domain medium by dielectric sensors (Ahmed et al., 2019). The cumulative complex electrical impedance of the media is determined by monitoring the currents and voltages influenced in the measuring rods by this field. The form and volume of the electric field are determined primarily by the form and size of the electrodes used for the sensors. Dielectric sensors are classified into several types based on the output signal, which include Time Domain Reflectometry (TDR), Capacitance or Frequency Domain Reflectometry (FDR), Time Domain Transmission (TDT), Amplitude Domain Reflectometry (ADR), and Phase Transmission sensors (PT), different in aspects of the use, maintenance, measurement requirements, accuracy, and cost (Vera et al., 2021).

2.4.1.1.1 Frequency Domain Reflectometry (FDR)

Frequency Domain (FD) or capacitive techniques use capacitance to measure the dielectric permittivity of a surrounding medium and operate at one single measurement frequency. When the amount of water changes in the soil, a probe will measure a change in capacitance due to the change in dielectric permittivity that can be directly correlated with a change in soil water content (Stacheder et al., 2009). **Figure 2.3** shows a picture of an FDR sensor.

Figure 2.3: FDR sensor (Sourced from: Garg et al., 2016)

2.4.1.1.2 Time Domain Reflectometry (TDR)

According to Stacheder et al., (2009), Time Domain Reflectometry (TDR) measures the bulk dielectric permittivity of soil, which includes the soil matrix, water, and air. It works by sending an electromagnetic (EM) pulse through a coaxial cable to a probe inserted into the soil. Part of the pulse is reflected at the probe due to impedance differences, while the rest travels to the end and is reflected back. The round-trip time of the pulse is measured to estimate soil properties. In homogeneous soils, the volumetric water content can be determined using an empirically derived calibration curve. A typical example of a TDR sensor is shown in **Figure 2.4**.

Figure 2.4: TDR soil moisture sensor (Sourced from: Garg et al., 2016)

2.4.1.2 Neutron moderation

Neutron moderation methods are categorized in to two types in order to measure the soil water content. The neutron scatters method is determined by the interplay of high energy (fast) neutrons in the soil with the nuclei of hydrogen atoms. The other technique determines the attenuation of gamma rays as they travel through soil. Both methods make use of portable devices to collect measurement invariance at fixed monitoring sites and necessitate accurate calibration, better with the soil where the devices are to be used (Vera et al., 2021). When properly calibrated, neutron probes are highly accurate. They not affected by salts, have a large measuring radius, and can measure at various depths. They are, however, extremely costly radiation hazards which can be hard to calibrate and install. Table *2.1* shows the advantage and disadvantages of dielectric and Neutron moderation sensors.

Table 2.1: Volumetric soil moisture sensors

Type of sensors	Advantages	Disadvantages
TDR	✓ Independent of soil texture temperature or salt content.	✓ Small sensing volume. ✓ Requires soil calibration. ✓ High cost.
FDR	✓ Can determine water content at any depth. ✓ Can provide the exact soil water content.	✓ Small sensing sphere. ✓ Require perfect conduct with soil to get accurate results
Resistive sensor	✓ Can provide the exact soil water content ✓ High precision when the soil's ionic concentration doesn't change	✓ Calibration is required as soil, and ionic concentrations change
ADR	✓ Because of standard circuitry, it is inexpensive. ✓ With proper calibration, it is accurate.	✓ Small sensing volume ✓ Soil specific calibration ✓ Measurement effect of air gaps and stones
TDT	✓ Accurate with large scale ✓ Because of standard circuitry, ✓ it is inexpensive.	✓ Soil disturbance during installation necessitates permanent installation.
PT	✓ Inexpensive ✓ Accurate with large scale ✓ Accurate with soil specific calibration	✓ Need to permanently installed ✓ Soil specific calibration

Neutron moderation	✓ Water can be measured at any phase ✓ Accurate with large volume at any depth	✓ High cost ✓ Hazard radiation ✓ Insensitivity to small variation
Gamma attenuation	✓ Can measure mean water content with depth as well as moisture content changes over time.	✓ High cost and difficult to use ✓ Measurement in highly stratified soil produces large errors ✓ Changes in soil bulk density have an impact.

(Source: Vera et al., 2021)

2.4.2 Tensiometric sensors

According to Bond & Hutchinson, (2006), Tensiometric sensors measure the potential of soil matrices. Tensiometers, electric resistance sensors, thermal conductivity sensors, and psychrometers are some of the most commonly used. The most common resistance types are electric and tensiometers. A tensiometer is a water filled tube designed to mimic the movement of a plant root. A porous cup with negative pressure (vacuum) measured at the other end is buried in the soil. As the soil dries, water is drawn out of the tensiometer, causing the pressure reading to fall, indicating that the soil moisture decreases. When the cup is irrigated, soil water returns and the pressure decreases. Tensiometers are sensitive to conditions in a large soil volume and are simple to install and maintain

2.4.2.1 Tensiometers

A tensiometer operates by allowing soil water to come into equilibrium with a reference pressure indicator through a permeable ceramic cup placed in contact with the soil. It measures the rate at which roots can pick up water from their surrounding media (Bond & Hutchinson, 2006). Drier soil has higher tension compared to the wetted soil. The soil water tension indicates the water availability better in the soil compared to the water content i.e. at the same water content, heavy soil holds back water and less is available to plants in comparison to a soil less media. Tensiometers are not affected by electroconductivity (EC) or soil temperature of the soil water solution because

salts move freely across the ceramic cup. On the other hand, tensiometers require frequent refilling with clean water especially when being used in dry environments where water is seeped out to the drier surrounding soil. Algae cleaning is another maintenance requirement as it makes the tension meter cavity to become greenish. A tight interface between the ceramic tip of the tensiometer and the soil is important, and this is ensured by using a single motion push of the sensor into the soil (Garg et al., 2016). Figure *2.5* shows a tensiometer which is installed with a porous cup at the end.

Figure 2.5: A tensiometer installed with a porous cup at the end (Sourced from: Sarkar et al., 2019)

2.4.2.2 Granular Matrix Sensors (GMS)

These are sensors that have been developed electronically to measure soil moisture and they operate on the same electrical principle as the gypsum bock and contain a reservoir of gypsum imbedded within the granular matrix. This design helps to minimize the influence of soil salinity on the resistance measurement which ensures more accurate moisture readings (Light et al., 2004). An example of a granular matrix sensor which is commonly used is the watermark soil moisture sensor meter showed in Figure *2.6*.

2.4.2.2.1 Watermark Soil moisture sensors

According to Chard, (2002), the watermark soil moisture sensors which are developed by the Irrometer Company (Riverside, CA, USA), are granular matrix sensors that similarly to a gypsum block since both are indirect sensors. This functioning makes the sensor highly resistant to corrosion when it comes in to contact with water of a high salinity level. It comprises of two concentric electrodes which are embedded within a reference matrix, encased in a synthetic membrane for enhanced durability. The sensor's robustness is further reinforced by a stainless-steel mesh and a rubber outer cover, making it more resilient than traditional gypsum blocks. Water movement between the soil and the sensor alters the electrical resistance between the electrodes, which can then be interpreted as soil water potential.

This type of sensor reads the resistance changes as the soil tension changes, which depends on the soil moisture content. As the soil moisture content changes, the electrical properties of the soil also change. This sensor measures from 0 to 239 kPa where the value of 0 kPa indicates that the soil reached saturation and the measurement of 239 kPa indicates that the soil is dry. In the mid-1990s, the Irrometer Company introduced improvements to the original Watermark model 200, resulting in the 200SS. This upgrade included refining the method for compacting the matrix material for better uniformity and replacing the plastic outer mesh with a stainless-steel version. The stainless-steel mesh in the 200SS features more and larger openings than the 200, increasing the contact surface area with the soil and enhancing response time.

The original model, 200 responded slowly during rapid drying or partial rewetting, especially at more negative water potentials. Additionally, variations in calibration were noted between different soils and sensors. While the 200SS offered advancements over the 200, such as improved accuracy and reduced variability among sensors, converting resistance readings (kΩ) to soil water potential (kPa) remained dependent on the specific sensor and soil type (Yu et al., 2021). According to (Chard, 2002), these sensors perform poorly in wet soil conditions (0 to -10 kPa).

Figure 2.6: Irrometer Model 200SS Watermark soil moisture sensor

(Source: water+mark+sensors)

2.4.2.2.2 Reading sensor output in a watermark sensor

Watermark sensors can be spot-read with a hand-held meter or monitored continuously with a datalogger in combination with a multiplexer. For the easy connection of a watermark sensor to a data logger, the sensor must be equipped with an in-line blocking capacitor. Figure *2.6* shows a watermark sensor with the digital meter.

2.4.2.2.3 Sensor calibration and monitoring

The watermark digital meter can be used to manually read the Watermark probes, The digital meter converts the digital output of the watermark from resistance (kΩ) to suction (kPa) using the non-linear calibration Equation *2.4* developed by Dr. Clinton Shock in 1998 (*wikipedia*, 2024).

$$kPa = \frac{-3.213 * \mathrm{R} \; - \; 4.093}{(1 \; - \; 0.009733 * \mathrm{R} \; - \; 0.01205 * \mathrm{T})}$$

Equation 2.4

where R is resistance in (kΩ) and T is temp centigrade. This calibration covers the range of 10 to 100 kPa and hence linear extrapolations are used below 10 and above 100 kPa (Chard, 2002). A fully wet calibrated watermark sensor measures 550 Ohms.

The measured resistance in the sensor is affected by temperature. A default temperature of 24 C can be used in the absence of temperature data, but a temperature sensor input can be used for increased accuracy. The calibration of Irrometer based on Equation *2.4*.

2.4.2.2.4 Sensor Power

Powering the watermark sensors can be most effectively done using AC because alternating current prevents the buildup of charge which could offset the readings and degrade the electrodes overtime (Orouskhani et al., 2023). However, if providing AC excitation is impractical, two alternatives can be used:

i. Pseudo-AC Short Pulse

This pulse is created by alternating the direction of current of a brief DC excitation for equal amounts of time. This approach alternates and isolates output pins, with the second pulse reversing the charge induced by the first. This leaves the sensor with no accumulated potential making the sensor ready to take the subsequent readings. Alternating can be achieved by switching the power and ground using hardware by setting a pin to low as the ground and switching the state of the two pins back and forth. As with the short pulse method, excitation should not exceed 50ms total and the measurement should be taken within 100 microseconds (Orouskhani et al., 2023).

ii. DC Short Pulse

When using DC without polarity switching, excitation should remain under 50 ms, and readings should be taken between 100 and 200 microseconds after applying the current. Delays beyond 200 microseconds can result in charge buildup, causing measurement errors and shortening electrode lifespan. To discharge any accumulated potential after reading, the sensor leads should be shorted or the powered lead should be connected to the ground for 30 seconds (Orouskhani et al., 2023).

2.5 Soil Moisture Placement and Installation

According to Orouskhani et al., (2023), several factors should be considerations when installing soil moisture sensors. The sensors should be installed between plants in a representative area within a row, preferably within the active root zone of the crops. Additionally, locations that are not representative of the majority field, such as hill tops, low lying areas, and the edge of the field should be avoided. For the case of a drip irrigation system, the sensors should be installed in the wetting zone of the soil as show in Figure *2.7*.

Figure 2.7: Demonstrated wetting zone under drip irrigation system using blue dye (Sourced from: Orouskhani et al., 2023)

2.6 Soil Water Tension

Soil Water Tension measures how tightly water is held in the soil due to capillary and adhesive forces (Shock et al., 2013). It is expressed in pressure units such as kilopascals(kPa) or centibars(cb). Higher SWT values indicate that water is less available to plants because it is more tightly bound to soil particles. This concept of soil water tension is essential in assessing the water availability to plants and optimizing the irrigation practices.

Soil Water Tension can be measured directly with tensiometers or indirectly with gypsum blocks, heat dissipation sensors, granular matrix sensors (e.g., Watermark sensors), porcelain resistance to air movement, thermocouple psychrometers, pressure plates and dielectric coupled media (e.g., MPS-1). Each instrument has specific strengths and limitations which makes them suitable for different applications and soil conditions. (Shock et al., 2013; Shock & Wang, 2010).

2.7 Communication Technologies

With the implementation of IoT devices, the choice of communication technology is very important because it will dictate the efficiency of achieving the intended operation. These technologies should be selected based on the specific environment where they will be set up (Obaideen et al., 2022). In this section, the various technologies that have been used in the world of smart irrigation. These technologies are a very crucial component when the IoT devices are deployed in the field because they determine how best and efficient the systems will be. Table *2.2* shows the different communication technologies which are used in smart irrigation systems.

Table 2.2: Different communication technologies employed in smart irrigation systems

Group	Technology	Frequency Bands	Max. Data Rate
Cellular	3G, 4G/LTE, 5G	380.2–389.8 MHz, 390.2–399.8 MHz, 410.2–419.8 MHz, 420.2–429.8 MHz	Upload 7.2 Mbps Download 2 Mbps
Wireless Personal Area Networks	IEEE 802.15.1-Bluetooth	2400–2483.5 MHz	Up to 3 Mbps
	BLE (Bluetooth Low-Energy)	2.400–2.4835 GHz	Up to 2 Mbps
RFID	Radio Frequency Identification (RFID)	Low Frequency: 125 or 134.2 kHz High Frequency: 13.56 MHz Ultra High Frequency: 868–956 MHz Microwaves: 2.45	UHF: Up to 640 kbps
Mesh Protocols	Zigbee	868–868.6 MHz, 902–9286 MHz, 2400 MHz	Up to 250 kbps

	Z-Wave	865.2 MHz, 869 MHz, 868.4 MHz, 868.40 MHz, 868.42 MHz, 869.85 MHz, 908.4 MHz, 908.42 MHz, 916 MHz, 919.8 MHz, 921.4 MHz, 919–923 MHz, 920–923 MHz, 920–925 MHz, 922–926 MHz	Up to 100 kbps
	Thread	Global: 2400–2500 MHz America, Australia: 902–928 MHz Europe: 868–868.6 MHz,	Up to 250 kbps
WiFI	IEEE 802.11a	5725–5875 MHz	Up to 54 Mbps
	IEEE 802.11b	2400–2500 MHz	Up to 11 Mbps
	IEEE 802.11g	2400–2500 MHz	Up to 54 Mbps
	IEEE 802.11n	2400–2500 MHz, 5725–5875 MHz	Up to 600 Mbps
Low-Power Wide Area Network (LPWAN)	NarrowBand IoT (NB-IoT)	Global: 1950 MHz, 2140 MHz, 1747.5 MHz, 1842.5 MHz, 897.5 MHz, 942.5 MHz, 455 MHz, 465 MHz	200 kbps

	Long-Term Evolution—Machine Type Communication (LTE-M)	Global: 1950 MHz, 2140 MHz, 1747.5 MHz, 1842.5 MHz, 897.5 MHz, 942.5 MHz, 455 MHz, 465 MHz	Upload peak rate of 5 Mbps Download peak rate of 10 Mbps
	Extended coverage GSM (EC-GSM)	Global: 385 MHz, 395 MHz, 415 MHz, 425 MHz, 454 MHz, 464 MHz, 482.4 MHz, 492,4 MHz, 707.2 MHz, 737.2 MHz, 785.2 MHz, 755.2 MHz, 813.7 MHz, 858.7 MHz	Downlink Peak Data Rate: 70 kbps (GSMK), 240 kbps (8PSK) Uplink Peak Data Rate: 70 kbps (GSMK), 240 kbps (8PSK)
	Sigfox	RC1: 868.130 MHz, 869.525 MHz RC2: 902.200 MHz, 905.200 MHz RC3: 923.200 MHz, 922.200 MHz RC4: 920.800 MHz, 922.300 MHz RC5: 923.300 MHz, 922.300 MHz RC6: 865.200 MHz, 866.200 MHz	100 or 600 bps
	LoRa—Low Power Wide Area Network (LoRaWAN)	Europe: 870 MHz, 863 MHz, 434 MHz, 433 MHz India: 867 MHz, 865 MHz	0.3 to 50 kbps
	MIOTY	868 MHz	

(Sourced from: Goap et al., 2018)

2.7.1 Cellular Communication

Cellular communication is based on mobile networks which are run by cellular service providers who use cellular towers to transmit data over long distances. The cellular communication offers high bandwidth and excellent distance coverage, making it suitable for applications that would be executed in areas of geographical distance. Examples include smart irrigation systems on remote pieces of land used for agriculture (Goap et al., 2018; Obaideen et al., 2022).

2.7.2 Wireless Personal Area Networks (WPAN)

According to Garc et al., (2020), WPAN short-range networks where wireless devices communicate within ranges of a few meters. For example, Bluetooth and Zigbee technologies are used to create connections between smartphones, sensors, and confined smart irrigation controllers near each other. Therefore, WPAN enables localized data communication and control within the smart irrigation set-up.

2.7.3 Radio Frequency Identification (RFID)

According to Shafi et al., (2019), Radio Frequency Identification uses radio waves to identify and track objects remotely by the use of RFID tags. The RFID tags can be attached to equipment, crops, or the containers, allowing the essence to be tracked and monitored while in motion or at a distance. Therefore, RFID can play several roles in smart irrigation, such as identifying the assets, managing inventory, and quality control, improving business operations, and resource management (Sciences, 2024).

2.7.4 Zigbee

Zigbee stands out as a low-power, low-data-rate wireless communication protocol that is suitable for smart irrigation systems, includes Zigbee. Zigbee is appropriate for connecting sensors and devices over short distances. Moreover, Zigbee can handle an infinite number of devices installed in throngs. One advantage of Zigbee over Wi-Fi and Bluetooth is that it can transfer a message through several devices and act as an intermediate data link (Goap et al., 2018).

2.7.5 Z-Wave

Operating within the sub-1GHz frequency range and optimized for home automation and IoT applications, Z-Wave provides a reliable range with excellent penetration through obstacles. While commonly used to connect smart home devices, this technology can also be effectively applied to smart irrigation systems, facilitating seamless interaction between components and ensuring efficient water management and irrigation control (Shafi et al., 2019).

2.7.6 Thread

Thread represents a low-power mesh networking protocol meticulously crafted for IoT applications. With its focus on security and reliability, Thread facilitates seamless communication over IPv6 networks, fostering interoperability among diverse devices and systems. This protocol is well-suited for smart irrigation setups demanding resilient and scalable communication infrastructure to support comprehensive monitoring and control functionalities (Goap et al., 2018).

2.7.7 Wi-Fi

Wi-Fi technology, renowned for providing high-speed internet access over short to medium distances, operates across the 2.4GHz and 5GHz frequency bands. Widely utilized for connecting computers, smartphones, and IoT devices to local networks, Wi-Fi finds application in smart irrigation systems for local connectivity purposes. It enables seamless integration of irrigation controllers with central networks, facilitating real-time data exchange and management (Shafi et al., 2019).

2.7.8 NarrowBand IoT (NB-IoT)

NB-IoT emerges as a cellular communication standard meticulously optimized for IoT applications. Operating within licensed spectrum bands, NB-IoT offers low-power, wide-area connectivity tailored for IoT devices. With its ability to facilitate long-distance communication while minimizing power consumption, NB-IoT proves ideal for smart irrigation systems, where devices need to communicate efficiently over extensive agricultural landscapes (Obaideen et al., 2022).

2.7.9 Long Term Evolution - Machine Type Communication (LTE-M)

LTE-M, a cellular communication technology purpose-built for IoT and M2M applications, delivers superior data rates and lower latency compared to traditional cellular networks. Suited for

real-time monitoring and control requirements, LTE-M ensures reliable connectivity in smart irrigation systems deployed across diverse agricultural settings, facilitating seamless integration and efficient data exchange over cellular networks (Ting & Chan, 2024b).

2.7.10 Extended Coverage Global System for Mobile Communication (EC-GSM)

EC-GSM, an extension of the GSM cellular standard, is engineered to enhance coverage and signal penetration. Operating within existing GSM spectrum, EC-GSM caters to IoT applications deployed in remote or challenging environments. In the context of smart irrigation, EC-GSM facilitates connectivity in rural or isolated areas, ensuring seamless communication between irrigation devices and control systems (Shafi et al., 2019).

2.7.11 Sigfox

Sigfox stands out as a low-power, wide-area network (LPWAN) technology designed specifically for IoT applications. Operating in unlicensed ISM bands, Sigfox provides long-range connectivity with minimal energy consumption. In smart irrigation setups, Sigfox technology enables efficient communication over extensive distances, ensuring reliable data exchange while minimizing energy usage for optimized resource management (Garc et al., 2020).

2.7.12 MIOTY

MIOTY is a low-power wide-area network (LPWAN) developed by the Fraunhofer Institute for Integrated Circuits, MIOTY utilizes telegram splitting technology to ensure robust, long-range communication with minimal energy consumption. Tailored for applications requiring reliable connectivity in challenging environments, such as smart agriculture and industrial IoT, MIOTY technology guarantees seamless data exchange and control within smart irrigation systems, enhancing operational efficiency and resource utilization (Garc et al., 2020).

The above IoT communication methods for irrigation can be divided into two main categories which are those designed for low-energy nodes that transmit small amounts of data over short distances, and those capable of transmitting large amounts of data over longer distances, which typically require higher energy consumption (Quy et al., 2022). Wi-Fi is one of the most commonly used and effective technologies due to its widespread availability and compatibility with many low-cost IoT devices. Although Wi-Fi has limitations in terms of coverage area, it remains an efficient solution overall. More recent advancements include Long Range (LoRa) and the Message

Queuing Telemetry Transport (MQTT) protocol. LoRa is notable for its extensive range, making it especially suitable for remote areas without traditional service coverage. On the other hand, MQTT is recognized for its low overhead and energy efficiency which is becoming more popular but has not yet been widely adopted in irrigation systems (Obaideen et al., 2022).

2.7.13 LoRa-Low Power Wide Area Network (LoRaWAN)

LoRa technology which is derived from Chirp Spread Spectrum (CSS), has emerged as a key solution for addressing challenges in IoT-based applications, particularly in smart irrigation. Its attributes are low power consumption, long-range coverage, and ease of deployment making it suitable for transmitting data from the sensor nodes to the servers/gateways, enabling the automation of irrigation systems (Ting & Chan, (2024). This technology encodes information using chirp pulses, similar to the communication methods of dolphins and bats. It is a proprietary spread spectrum modulation technique developed by Semtech (Bor et al., 2016) and is increasingly used in low-power, battery-operated IoT systems that transmit small data packets over long distances according to Devalal & Karthikeyan (2018).

The technology provides a long-range communication link at the physical layer, which is standardized and enhanced by LoRaWAN. The LoRaWAN specification, standardized and open-sourced by the LoRa Alliance, defines the network architecture and communication protocol. Its star topology significantly reduces power consumption and extends battery life compared to conventional mesh networks. The LoRa network comprises four key components: LoRa Nodes (endpoints), Gateways, the Network Server, and the Application Server (Bor et al., 2016). Figure *2.8* shows the LoRaWAN architecture which is operated by the LoRa wireless technology.

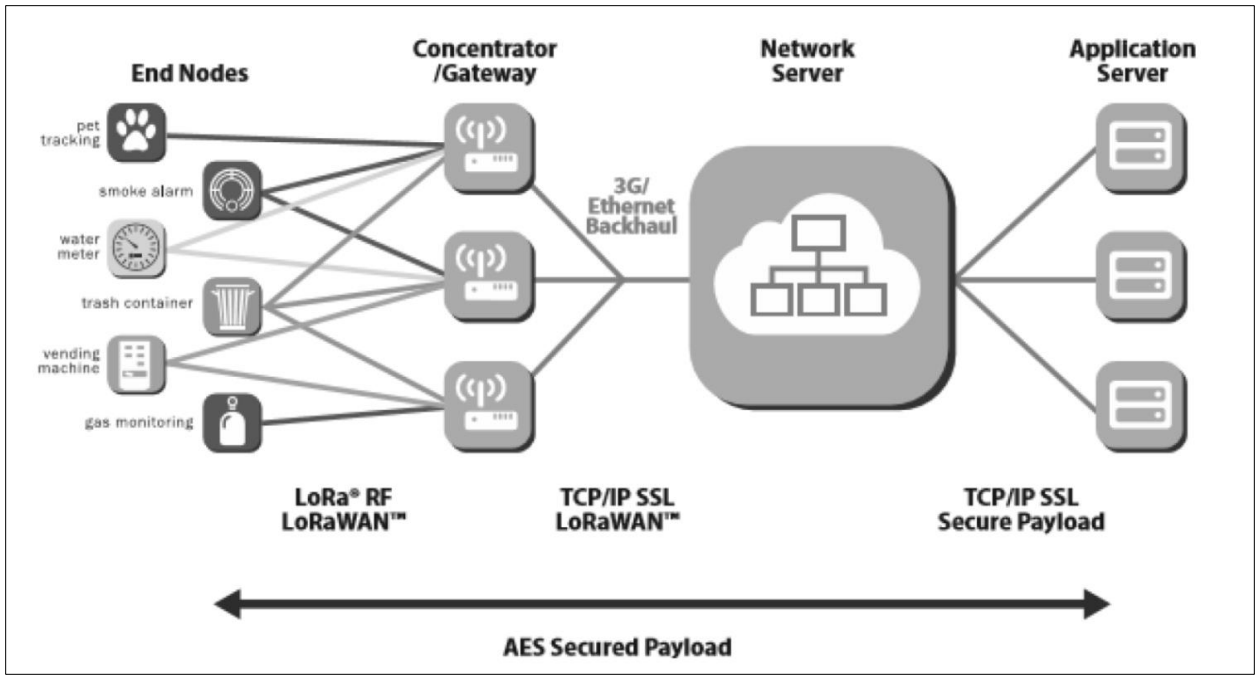

Figure 2.8: LoRaWAN architecture (Sourced from: Devalal & Karthikeyan, 2018)

2.7.13.1 Characteristics of the LoRaWAN technology

LoRa technology offers long-range communication capabilities of up to 10 miles in line-of-sight conditions, making it ideal for wide-area applications. It supports long battery life of up to 10 years, especially when operating in Class A or Class B modes, which help conserve power by accepting higher downlink latency. The technology is cost-effective, with low device and maintenance costs, and operates on license-free radio spectrum, though regional regulations must be observed. Despite its low power consumption, LoRa has a limited payload size ranging from 51 to 241 bytes depending on the data rate, which typically varies between 0.3 Kbit/s and 27 Kbit/s, with a maximum payload of 222 bytes (Sourced from: Devalal & Karthikeyan, 2018).

2.7.14 LoRaWAN based smart irrigation systems

Systems running on LoRa technology all run on the basic principles. It requires the interaction of three major components which are:

2.7.14.1 LoRaWAN Gateway

The main purpose is to provide a communication path between LoRa devices and Network server.

2.7.14.2 LoRaWAN sensor node

This component collects field data and sends it to the network server via a gateway using an Ebyte SX1276 LoRa module (Figure *2.9*), which supports LoRaWAN connectivity. Since the SX1276 operates at 3.3V logic and the Arduino Uno uses 5V logic, direct connection could damage the module. Therefore, a TXS0108E logic level shifter is required to safely handle the bidirectional communication between the Arduino Uno and the SX1276 module.

Figure 2.9: Ebyte SX1276 LoRa module

Figure 2.10 illustrates the TXS0108E logic level shifter, a device used to convert 5V signals down to 3.3V, making it suitable for 3.3V logic devices, and stepping up 3.3V to 5V when needed.

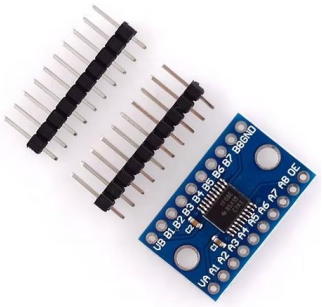

Figure 2.10: TXS0108E logic level shifter

2.7.14.3 LoRaWAN network server

This a critical component of a LoRaWAN architecture and it is the central management system that coordinates the communication between devices like sensors, gateways and application servers. Additionally, it aids data analysis, storage of the data and issuing of irrigation decisions.

2.8 Arduino microcontrollers

The Arduino microcontroller is an open-source platform introduced in 2005, designed for easy programming and interaction with sensors. It includes both hardware (the development board) and software (Arduino IDE), and supports programming in C/C++. The boards typically use 8-bit AVR or 32-bit ARM microcontrollers by Atmel (Ismailov, 2022). Arduino boards feature input/output pins for data handling and can connect to the internet. ESP boards are a type of microcontroller with built-in Wi-Fi capability, functioning either as a client or server. In this project, Arduino is used to read soil water tension, display it on an LCD, and send data via a LoRa module. Figure *2.11* shows a well labelled diagram of an Arduino microcontroller board.

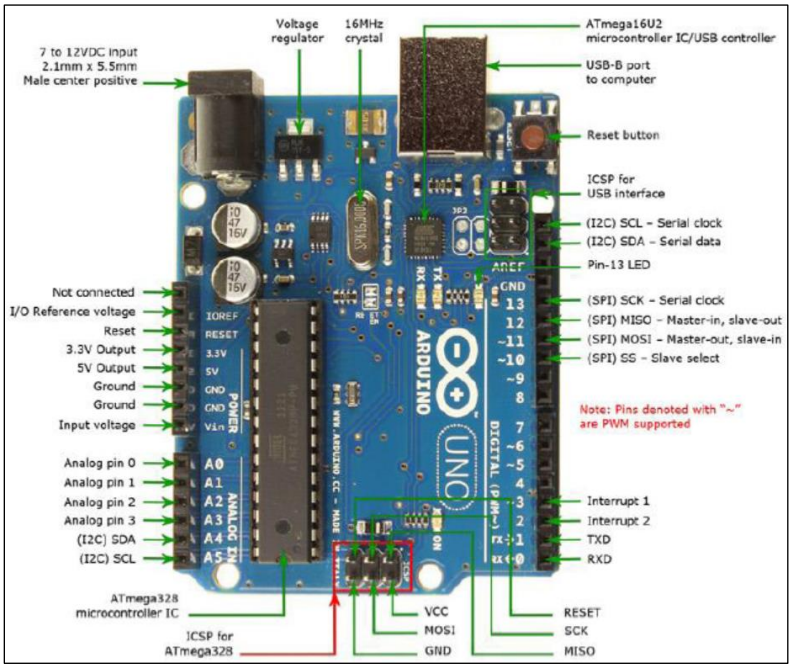

Figure 2.11: A labelled diagram of an Arduino board (Sourced from: Ismailov, 2022)

2.8.1 Components of an Arduino microcontroller

Arduino boards can be categorized into two main elements which are the hardware and software. The hardware comprises of several essential components which all serve different functions. These components include: the microcontroller, external power supply, USB port, reset buttons, and pins. The pins include analog and digital pins, power and ground pins (Ismailov, 2022).

2.9 System Testing

These are the tests which will be done to assess the robustness of the sensor node while it is carrying out its functions. The strength of the transmitted signals is measured using the Received Signal Strength Indicator (RSSI) and Signal to Noise Ratio (SNR)

2.9.1 Received Signal Strength Indicator (RSSI)

RSSI is the measure of the power present in a received radio signal and is expressed in decibels relative to a milliwatt (dBm). The RSSI values indicate how strong or weak the received signal is and this is done when the receiver measures the signal's strength at its end, with the RSSI inversely proportional to the distance and influenced by the environmental factors like obstacles and interreference (Smolau, 2009).

2.9.2 Signal to Noise Ratio (SNR)

According to Smolau, (2009), Signal-to-Noise Ratio (SNR) represents the ratio between the power of the received signal and the power of the noise floor. The noise floor consists of all the unwanted, interfering signal sources that can distort the transmitted signal, potentially leading to re-transmissions. The variations in SNR over time are illustrated in Figure *2.12* below.

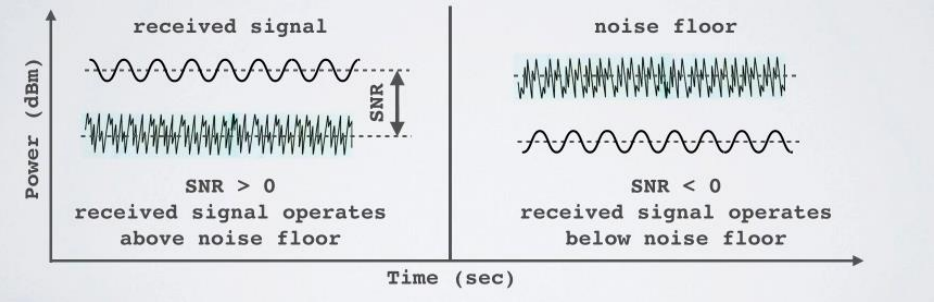

Figure 2.12: SNR variations with time (Sourced from: Smolau, 2009)

Normally the noise floor is the physical limit of sensitivity, however LoRa works below the noise level. The typical LoRa SNR values are between -20dB and +10dB. However, a value closer to +10dB means the received signal is less corrupted. Additionally, LoRa can demodulate signals which are -7.5 dB to -20dB below the noise floor.

CHAPTER THREE: MATERIALS AND METHODS

This describes the various steps that were done during the completion of this project.

3.1 Description of the Study Area

The study was conducted at Makerere University Agricultural Research Institute Kabanyolo (Figure 3.1). MUARIK is located on spatial coordinates 0˚27'60"N, 32˚36'24" E at an altitudinal range of 1250 m to 1320 m above mean sea level. The study site is within the administrative boundaries of Nangabo Sub County, Wakiso district and about 14 km north of Kampala, Uganda's capital city. Kabanyolo is part of the Lake Victoria basin that receives an average annual precipitation of 1218 mm with dry seasons in June and July, as well as December to February. MUARIK experiences a tropical climate with average high temperatures of 28.5 ºC and mean low temperatures of 14ºC (Okiror et al., 2017). Figure *3.1* shows the location of the study area.

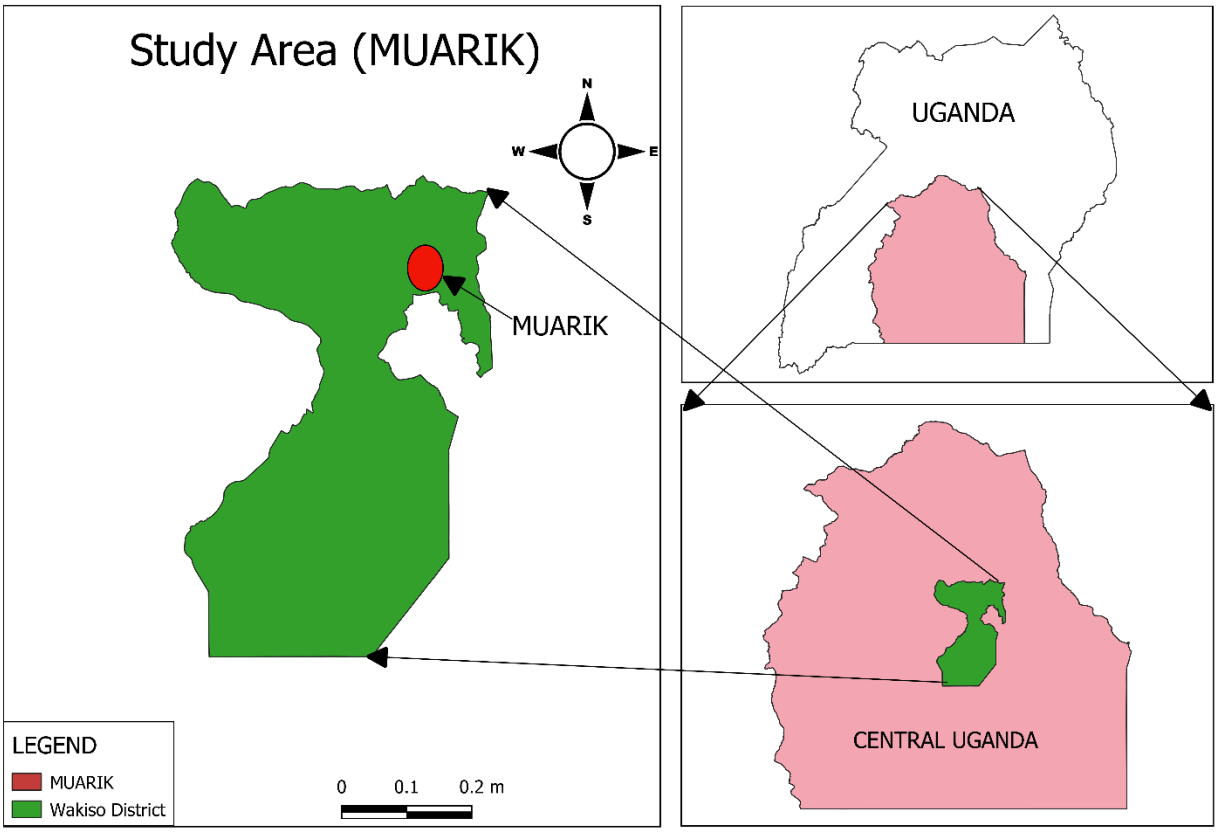

Figure 3.1: Map of Uganda showing the location of MUARIK.

The test field where the Solar powered, LoRa-based soil moisture sensor node was installed covers an area of 0.14 acres and is located at the MUARIK DABE demonstration irrigation site as shown in Figure *3.2* below.

Figure 3.2: Site location of the test field

3.2 Design and development of a solar-powered, LoRa-based soil moisture monitoring node.

3.2.1 Design considerations considered in building the sensor node

This subsection outlines the design and specifications of the equipment that were used in setting up and constructing the sensor node.

3.2.1.1 Long-Range communication

In this project, the SX1276 LoRa transceiver module was used due to its compatibility with LoRaWAN networks. It offers a communication range of up to 15 km, making it highly suitable for rural or semi-urban environments where the range requirements exceed those of Wi-Fi or Bluetooth Low Energy (BLE). Additionally, the module is ideal for battery and solar-powered

systems due to its low power consumption. Moreover, the SX1276 supports LoRaWAN 1.0.3, making it well-suited for both public and private LoRaWAN applications.

3.2.1.2 Energy supply system

The design of the solar supply system entailed the following components:

- 15 W solar panel
- First buck converter (solar to battery charging voltage)
- 3S lithium-ion battery pack
- 3S battery management system (BMS)
- Second buck converter (battery to Arduino operating voltage)
- Arduino Uno microcontroller

This configuration enables autonomous operation of the Arduino platform in remote locations without access to grid power, with sufficient energy storage to maintain operation during periods of limited sunlight.

Component specifications and design calculations

i. Solar panel specifications

The specifications of the solar panel which were used in this project are showed in Table *3.1* below.

Table 3.1: The solar panel specifications

Specifications	Values
Maximum power	15W
Voltage at Maximum Power (Vmp)	17.2V
Current at Maximum Power (Imp)	0.87A

Open Circuit Voltage (Voc)	21.6V
Short Circuit current (Isc)	0.98A
Maximum System Voltage	DC 1000V
Maximum Series Fuse Rating	3A
Dimensions	430mm × 360mm × 17mm

ii. First buck converter (solar to battery)

This converter steps down the solar panel voltage to the appropriate charging voltage for the 3S lithium-ion battery pack. Figure *3.3* shows the type of buck converter which was used in this project.

Figure 3.3: A buck step-down converter

The chosen specifications for this component are as follows: a typical input voltage of 17.2 V, with a maximum open-circuit voltage (Voc) of up to 21.6 V; an output voltage of 12.6 V, suitable for fully charging a 3S lithium battery pack; and a required output current of at least 0.8 A.

Calculations:

- Power from solar panel: 15W maximum
- Converter efficiency (estimated): 85%
- Expected output power: 15W × 0.85 = 12.75W
- Output current capacity: 12.75W ÷ 12.6V = 1.01A

The selected specifications used in this project include a minimum input voltage of 22 V, an adjustable output voltage set to 12.6 V, a current rating of at least 1.5 A, and a power conversion efficiency of 85% or higher.

iii. Battery Storage system

The system consists of three lithium-ion batteries connected in series, each with a capacity of 6800 mAh. Each cell has a nominal voltage of 3.7 V and reaches 4.2 V when fully charged, resulting in a total pack voltage of 11.1 V nominal and 12.6 V when fully charged.

iv. Battery Management System

The Battery Management System (BMS) is responsible for safeguarding and balancing the battery pack. For this project, the BMS was selected based on its ability to provide the following essential functions: overcharge protection (cutoff at 4.2 V per cell), over-discharge protection (cutoff at 3.0 V per cell), cell balancing, and short-circuit protection. Figure *3.4* shows the type of 3S BMS that was used incorporated in the 3S lithium-ion battery pack.

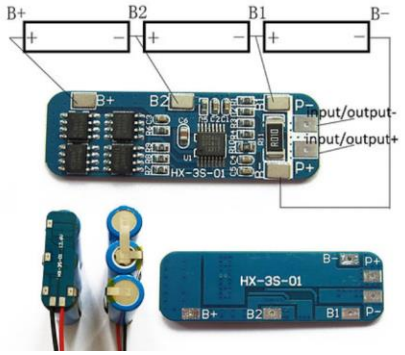

Figure 3.4: A 3S Battery Management System

v. Second buck converter (Battery to Arduino)

This converter is used to step down the battery pack voltage to a suitable level for powering the Arduino Uno. The design specifications include: an input voltage range of 9.0 V to 12.6 V (matching the battery pack output), an output voltage of 9 V (optimal for the Arduino Uno), and a required current capacity of 50–200 mA, which corresponds to the typical power consumption of the Arduino.

Calculations:

- Arduino power consumption: 9V × 0.2A = 1.8W (maximum)
- Converter efficiency (estimated): 85%
- Required input power: 1.8W ÷ 0.85 = 2.12W
- Input current from battery: 2.12W ÷ 11.1V = 0.19A (at nominal voltage)

The specifications selected for this project include a minimum input voltage of 13 V, an adjustable output voltage set to 9 V, a current rating of at least 500 mA, and a power conversion efficiency of 85% or higher.

Battery Runtime Analysis

Runtime calculations were based on the actual battery capacity:

For 6800mAh (6.8Ah) batteries:

- Energy storage: 6.8Ah × 11.1V = 75.48Wh
- Usable energy (80% Depth of Depletion): 60.38Wh

- Runtime with Arduino only (50mA): 60.38Wh ÷ 0.45W = 134.2 hours (5.6 days)
- Runtime with moderate load (150mA): 60.38Wh ÷ 1.35W = 44.7 hours (1.9 days)
- Runtime with full load (200mA): 60.38Wh ÷ 1.8W = 33.5 hours (1.4 days)

Charging Time Analysis

Solar Panel Output:

- Maximum power: 15W
- Charging power after converter: 15W × 0.85 = 12.75W
- Charging current at 12.6V: 12.75W ÷ 12.6V = 1.01A (theoretical)

Charging Time Estimates:

For 6800mAh (6.8Ah) batteries:

- Full charge requirement: 6.8Ah
- Charging time (ideal conditions): 6.8Ah ÷ 1.01A = 6.73 hours
- Charging time (real-world condition, 70% solar efficiency): 6.73h ÷ 0.7 = 9.61 hours (approximately one full day of sunlight)

In summary, the system comprises three main stages: energy harvesting, storage, and utilization. A 15W solar panel captures solar energy, which is regulated by a buck converter to match the charging requirements of the battery pack. This energy is stored in a 3S lithium-ion battery pack, safeguarded and managed by a 3S Battery Management System (BMS). Finally, another buck converter steps down the stored battery voltage to a suitable level for powering the Arduino Uno microcontroller, where the energy is put to use.

3.2.2 Sensor Selection, installation and calibration

3.2.2.1 Sensor Selection

The Irrometer 200SS Watermark sensor, a tensiometric soil moisture sensor, was selected for this study due to its accuracy, affordability, ease of installation, soil compatibility, and proven effectiveness in irrigation scheduling. It measures soil moisture tension which indicates the effort crops need to extract water from the soil.

3.2.2.2 Sensor Installation

The soil moisture sensors should always be installed at an appropriate depth for the specific crop and soil type. In this project, the Irrometer 200SS Watermark sensor was installed within the active root zone of the crop by the help of a soil auger. Figure *3.5* shows the installation of the watermark sensor in the active root zone. Cabbage was used as a representative example, with a typical root depth of 30 cm below the ground surface. The sensor was positioned vertically in the soil, ensuring that the probe was in direct contact with the surrounding soil for accurate moisture readings (Yu et al., 2021).

Figure 3.5: Installation of the watermark sensor in the active root zone of the crop.

3.2.2.3 Sensor Calibration

Soil moisture sensors should always be calibrated to the specific type of soil in which they will be installed to ensure accurate measurements. Calibration involves comparing the sensor's readings to actual soil moisture levels determined using a standard method which inn this case is the gravimetric method. Based on this comparison, the sensor is then adjusted to improve the accuracy of its readings. In this study, the soil water tension values recorded by the sensor were compared to those obtained using the gravimetric method, which is widely regarded as the most accurate technique for measuring soil moisture.

The following procedure for calibration was followed:

The gravimetric method was used as the reference for calibrating the watermark sensors which involved determining the soil moisture content by measuring the mass loss due to water evaporation during oven drying. The moisture content is then expressed as grams of water per 100 grams of oven-dry soil. The calibration process involved the use of several apparatus, including a precision balance (±0.001 g or better), a drying oven capable of maintaining 105 °C ± 5 °C, the Watermark sensor, a bucket, aluminium foil, a measuring cylinder, a 2 mm sieve, and sample can. Before calibration, the collected soil samples were pre-treated by drying them in an oven at a maximum temperature of 40 °C for 24 hours to eliminate excess moisture while preserving soil properties. The dried soil was then passed through a 2 mm sieve to ensure uniform particle size distribution. To prevent the reabsorption of moisture, the sieved soil was allowed to cool inside the switched-off oven with the door closed. The cooled soil was transferred to a bucket and thoroughly mixed. A portion of the soil was then extracted and this is where the watermark sensor was inserted in order to obtain the initial soil moisture tension reading.

Next, a clean, empty can was placed on a precision balance and its weight was recorded as the "mass of can." The sensor remained inserted in the soil within the can, and three readings were taken at 5-second intervals to obtain an average sensor value for the sample. A small amount of soil was then added to the can, and the total weight was recorded as the "weight of wet soil + can." To generate a range of moisture levels for calibration, small quantities of water were incrementally added to the soil in the bucket. After each addition, the soil was mixed thoroughly to ensure even distribution of moisture. In total, forty-one soil samples with different moisture levels were prepared, labelled, and placed in the oven at 105 °C ± 5 °C for 24 hours. After drying, the samples were cooled and their weights were recorded under the "Mass of dry soil + container" column. This entire process was repeated two more times for each sample to ensure the accuracy and reliability of the calibration results.

Th gravimetric water content (W%) for each sample was collected using the following equation (Equation *3.1*)

$$W\% = \frac{Mw-Md}{Md-Mc} \text{ x } 100$$

Equation 3.1

Where:

Mc = Mass of container (g)

Mw = Mass of wet soil sample plus the container (g)

Md = Mass of dry soil sample plus the container (g)

The volumetric water content was then derived from the gravimetric water content by multiplying it by the bulk density of the soil, obtained by measuring the ratio of the mass of dry soil to its volume.

A graph of gravimetric water content was plotted against the watermark soil water potential and a calibration curve was obtained which gave me the calibration equations.

3.2.2.4 Sensor Validation

For the validation process, the steps closely follow those used in calibration, utilizing the gravimetric method. The primary difference is that soil moisture tension values are directly collected from the field. Readings were taken from the calibrated watermark sensor, and simultaneously, soil samples were collected from the same locations as the sensor readings. These soil samples were then analyzed using the gravimetric method to determine their moisture content. The moisture tension readings obtained from the watermark sensor and the gravimetric method were tabulated. Figure *3.6* shows the station installed in the field, which includes a perforated bucket filled with soil containing the calibrated Watermark sensor. Soil samples were collected at the same time the sensor readings were taken.

Figure 3.6: Station used for obtaining the validation results

3.2.3 Reading of soil moisture tension from the watermark sensor

A C++ code was written in the Arduino IDE which incorporated the calibration equations derived from the calibration curve. Initially, soil water tension readings were obtained using a laptop, with the values displayed on the Arduino IDE console. Figure *3.7* shows a picture of me reading the soil water tension values from the watermark sensors using my laptop which worked perfectly well.

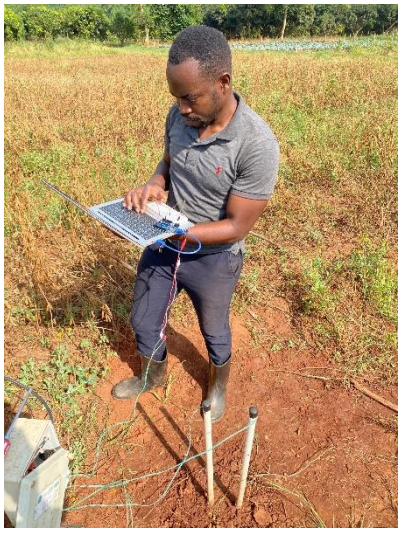

Figure 3.7: Reading of the soil water tension using my laptop in the Arduino IDE console.

After ensuring that the code was working efficiently well, an acrylic casing of a 2.5mm thickness was designed using the adobe illustrator and laser cut. This acrylic housing protected the delicate electronic components such as the 20 by 4 LCD screen, Arduino uno microcontroller board, the 3 lithium-ion pack, the SX1276 LoRa module, TXS0108E logic level shifter, 3S battery managements system and the two buck converters from harsh weather conditions like rainfall and too much sunlight. Figure *3.8* shoes the green acrylic housing that was used to store all the delicate electronic components.

Figure 3.8: The acrylic housing

3.2.4 Assembling and building of the sensor node

After confirming that all components and preparatory tasks required for the proper functioning of the sensor node were completed, the assembly process began to construct the full sensor node system. The following steps were carried out systematically:

Firstly, an 8-foot-tall hollow steel pole was laid on the ground to begin the setup. An acrylic casing, meant to house the electronic components, was mounted onto the pole. Following this, the solar panel with dimensions of 430 mm × 360 mm was installed on a rectangular frame at the top of the pole. The height of the pole was intentionally designed to be 8 feet to avoid interference from plant biomass, such as leaves or overhanging branches, which could obstruct solar exposure or the LoRa communication.

Next, a 60 cm-deep pit was dug at the designated site for installation. The pole, now fitted with the acrylic casing and solar panel, was inserted into the pit. Soil was backfilled around the base of the pole to provide initial support. To firmly secure the pole, stones, sand, and cement were added to the pit. The backfilling continued until the surface of the filled pit was level with the surrounding ground, ensuring stability and durability of the erected structure. Figure *3.9*, Figure *3.10* and Figure *3.11* show some of the procedures which I followed in building the sensor node.

Figure 3.9: Inserting the acrylic casing on to the steel pole

Figure 3.10: Setting up the solar panel on top of the rectangular frame situated at the top of the pole

Figure 3.11: Back filling the dug pit having the erected 8ft tall steel pole

3.3 Programming and configuration of the sensor node for accurate real-time soil moisture monitoring and seamless communication with the existent smart LoRa-based irrigation system

3.3.1 Programming of the sender node

After the design and physical development of the solar-powered LoRa-based soil moisture monitoring sensor node, the next phase was programming and system integration. This involved incorporating the LoRa wireless communication feature into the sensor node by interfacing a LoRa module with the Arduino Uno microcontroller so that communication can be initiated between the sensor node and the existent LoRa-based smart irrigation system.

For this project in particular, the Ebyte SX1276 LoRa transceiver module which was developed by Semtech was selected because of its compatibility with the LoRaWAN (LoRa Wireless Area Network) infrastructure and its strong transmission capabilities. It featured a high-performance helical antenna, enabling the reliable data transmission over distances of up to 5 kilometres, making it ideal for very large agricultural environments. The module operates at a frequency of 868 MHz, which aligns well with frequency regulations and LoRaWAN compatibility in Uganda. To configure the module for transmission, specific parameters were programmed into the code which effectively set up the SX1276 module to function as a transmitter.

However, a technical challenge needed to be addressed: the SX1276 operates on 3.3V logic, while the Arduino Uno uses 5V logic. This means that directly connecting the two equipment would risk damaging the LoRa module. As a precaution, I bridged this gap using a logic level shifter, TXS0108E, which was introduced between the Arduino Uno board and the SX1276. This component efficiently stepped down the 5V signals from the Arduino uno board to 3.3V levels required by the LoRa module since the two components would be having bi-directional communication. Figure *3.12* shows the circuit diagram of the pin connections that I followed when connecting the Arduino Uno, TXS0108E logic level shifter and the SX1276 LoRa module.

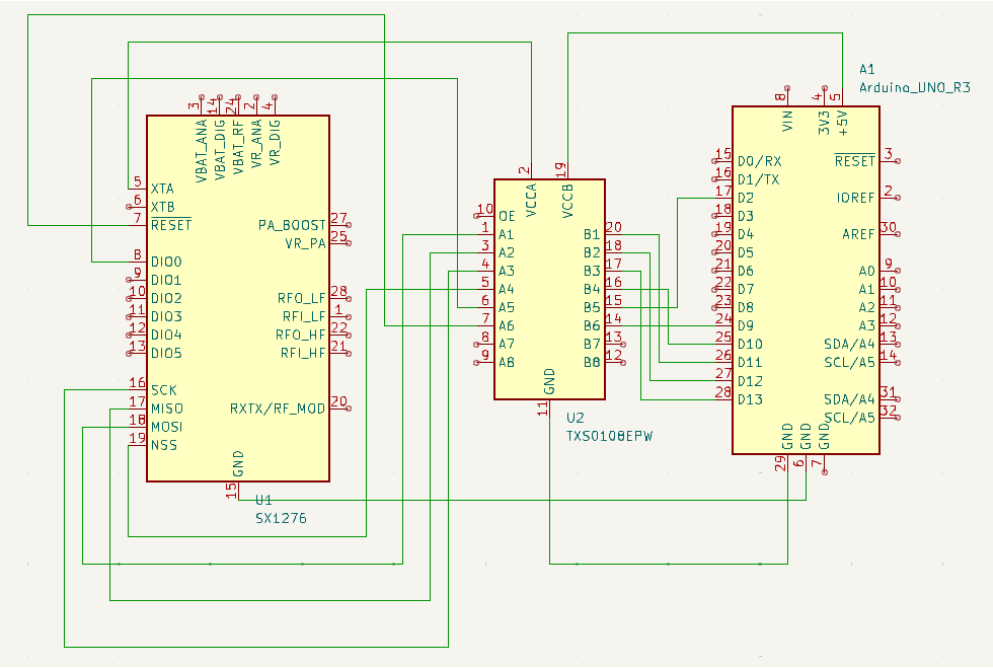

Figure 3.12: Circuit diagram showing pin connections between the Arduino Uno, TXS0108E logic level shifter and the SX1276 LoRa module

After completing the hardware connections, a C++ script was developed within the Arduino IDE to command the transmission of soil water tension data packets from the sensor node to the LoRa gateway. This script was thoughtfully designed to initiate data logging every 60 seconds, but only when the system is active. The 60-second delay serves a critical purpose of giving ample time to the watermark sensor to equilibrate with its surrounding soil conditions and to the data loss in mid-air since a lot of data is generated, thereby ensuring that the captured readings reflect the most accurate measure of soil moisture tension. Figure *3.13* and Figure *3.14* show the Arduino scripts that were uploaded on to the Arduino which was responsible for giving tasks to the sensor node.

```
#include <lmic.h>, <hal/hal.h>, <SPI.h>, <Wire.h>, <LiquidCrystal_I2C.h>, <math.h>
LiquidCrystal_I2C lcd(0x27, 20, 4);  // LCD display

// PROGMEM labels for efficient LCD display
const char LABELS[] PROGMEM = {...};  // Includes all string labels like "Res:", "Tension:", etc.

void printProgmemStr(const char* str);  // Print PROGMEM strings on LCD

// Sensor and LoRaWAN constants
#define num_of_read 5
const int Rx = 10000;
const uint8_t default_TempC = 24, SupplyV = 5;
const float cFactor = 1.1;
const uint16_t open_resistance = 35000, short_resistance = 200;
const uint8_t short_CB = 240, open_CB = 255;

// OTAA credentials in PROGMEM
static const u1_t PROGMEM APPEUI[8] = {...};
static const u1_t PROGMEM DEVEUI[8] = {...};
static const u1_t PROGMEM APPKEY[16] = {...};
void os_getArtEui(u1_t* buf), os_getDevEui(u1_t* buf), os_getDevKey(u1_t* buf);

// LoRa and sensor setup
static uint8_t soildata[4];
static osjob_t sendjob;
const unsigned TX_INTERVAL = 60;  // Send every 60 sec
const lmic_pinmap lmic_pins = {.nss=10, .rst=9, .dio={2, 3, LMIC_UNUSED_PIN}};
const uint8_t WM_PIN1=6, WM_PIN2=7, WM_ANALOG=A1;

// Event handler for LoRaWAN states
void onEvent(ev_t ev) {
    // Handles EV_JOINING, EV_JOINED, EV_JOIN_FAILED, EV_TXCOMPLETE, EV_TXSTART
    // Updates LCD and schedules next send
}
```

Figure 3.13: The first segment of the sender code

```
    updateLCD(resistance, abs(cb));
    soildata[0] = resistance & 0xFF;
    soildata[1] = (resistance >> 8) & 0xFF;
    soildata[2] = abs(cb) & 0xFF;
    soildata[3] = (abs(cb) >> 8) & 0xFF;
    LMIC_setTxData2(1, soildata, sizeof(soildata), 0);
}

// Arduino setup
void setup() {
    Wire.begin(); lcd.init(); lcd.backlight(); lcd.clear(); printProgmemStr(LABEL_TITLE);
    pinMode(WM_PIN1, OUTPUT); pinMode(WM_PIN2, OUTPUT);
    digitalWrite(WM_PIN1, LOW); digitalWrite(WM_PIN2, LOW);
    os_init(); LMIC_reset(); do_send(&sendjob);
}

// Arduino main loop
void loop() {
    os_runloop_once();
}

// Update LCD with resistance and CB value, with status like WET/MOIST/DRY
void updateLCD(uint16_t resistance, int cb_value) {
    // Clears and prints resistance, CB value, and status message
}

// Reads analog sensor values and calculates average resistance
uint16_t readWMsensor() {
    // Alternates excitation pins, averages readings, calculates resistance
    return (uint16_t)avg_resistance;
}

// Converts resistance to centibar (soil moisture tension) using temp correction
int myCBvalue(uint16_t res, uint8_t TC, float cF) {
    // Handles OPEN/SHORT cases, uses Watermark sensor equations for CB
    return WM_CB;
}
```

Figure 3.14: The second segment of the sender code

3.3.2 Programming of the gateway

On the receiving end, the sensor node was registered in to the gateway using the **Add Device** option within the ChirpStack software and it was given the name “Arthur’s LoRa Sensor Node”. This step was essential to initiate and enable seamless communication between the sensor node and the gateway. Following this, the join credentials were generated by ChirpStack: namely the **DevEUI, AppEUI,** and **AppKey**. These unique identifiers, all in hexadecimal format, were

required for Over-The-Air Activation (OTAA) and had to be configured in the sender's Arduino code to ensure secure and compatible communication.

While integrating these credentials into the Arduino sender code, specific formatting was necessary. The **DevEUI** and **AppEUI** values were each prefixed with "Ox" and written in reverse byte order i.e. the last byte in the original string was written first, and the first byte last. In contrast, the **AppKey** was entered in the exact order as provided by ChirpStack, with each byte simply prefixed by "Ox". Table *3.2* shows the ChirpStack credentials that were used to ensure compatibility between the LoRa sensor node and the gateway.

Table 3.2: ChirpStack credentials that were fed in to the sender code.

Criteria	**Values**
DEVEUI	a996c70cd58d9f2f
APPEUI	0cd5725355bce86b5
AppKey	947bc4ee529d0e6afa2a1309cc96067c

After the successful integration of the two devices, a JavaScript-based decoder script was developed and uploaded in to the ChirpStack software, which manages the LoRa gateway. The primary role of the JavaScript codec was to interpret the incoming data packets by converting the raw hexadecimal uplink messages transmitted from the sensor node into readable soil water tension values. These values offer real-time insights into the soil's moisture status, enabling seamless monitoring and analysis, as they are continuously logged to the gateway where they serve as the basis for generating data-driven irrigation schedules. Figure *3.15* shows the JavaScript code that was developed with an aim of translating the uplinked hexadecimal messaged in to readable format.

```javascript
function decodeUplink(input) {
  var decoded = {};
  var warnings = [], errors = [];

  if (input.bytes.length < 4) {
    errors.push("Invalid payload length");
    return { data: decoded, warnings, errors };
  }

  var resistance = input.bytes[0] + (input.bytes[1] << 8);
  var cbValue = input.bytes[2] + (input.bytes[3] << 8);

  decoded.resistance_ohms = resistance;
  decoded.soil_tension_cb = cbValue;

  if (cbValue === 240) {
    decoded.status = "SENSOR_SHORT";
    warnings.push("Sensor short detected");
  } else if (cbValue === 255) {
    decoded.status = "SENSOR_OPEN";
    warnings.push("Sensor open or not present");
  } else if (cbValue < 10) {
    decoded.status = "WET";
  } else if (cbValue < 30) {
    decoded.status = "MOIST";
  } else if (cbValue < 60) {
    decoded.status = "MODERATE";
  } else if (cbValue < 100) {
    decoded.status = "DRY";
  } else {
    decoded.status = "VERY_DRY";
  }

  return { data: decoded, warnings, errors };
}
```

Figure 3.15: The JavaScript codec that was used to decode the uplink messages sent from the sensor node

Figure 3.16: Programming the LoRa gateway using the Arduino IDE in my laptop

After this setup, the sensor node could clearly be seen on the dashboard of the gateway as an active device. Figure *3.16* shows the gateway dashboard which shows the devices that have been connected to it such as the “Arthur’ LoRa Sensor Node” and “Strega smart valve”.

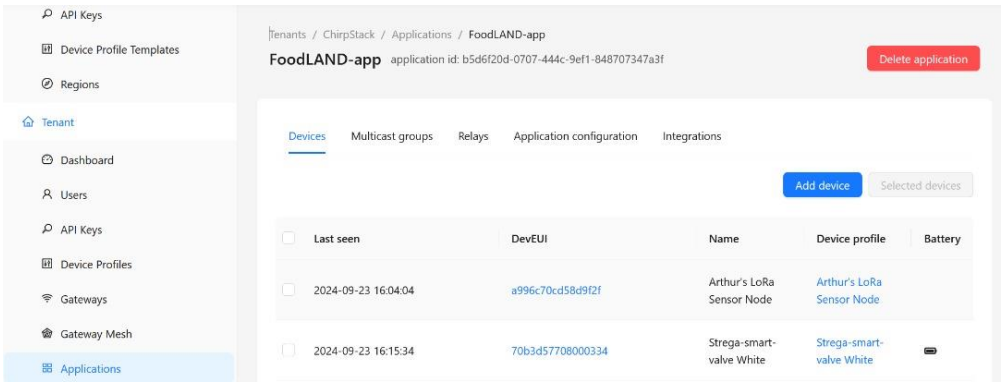

Figure 3.17: The gateway dashboard showing the devices that are connected to it.

3.3.3 Testing of the robustness of the LoRa wireless network

The strength of the LoRa wireless network was evaluated at two different locations within MUARIK: the Farm Shelter and the Continuing Agricultural Education Centre (CAEC). At each location, the LoRa gateway was set up to receive uplink messages transmitted from the sensor node.

At the Farm Shelter, which offers a clear line of sight with minimal physical obstructions, the uplink messages were received with minimal interference, demonstrating strong and stable communication. In contrast, when the gateway was placed at the CAEC, the uplink messages encountered significant interference due to several obstacles, including trees and buildings, which affected the signal quality. Figure *3.18* shows a Google Earth image of the different radii of the two test places from the Sensor node which is installed in the field.

Figure 3.18: Google earth image showing the two test sites

The following procedure was followed during the setup and testing process:

1. The sensor node was first installed in the field and powered on.
2. The LoRa gateway was then set up at the designated test location.
3. Once operational, the sensor node began transmitting uplink messages over the LoRaWAN network to the gateway. These messages were received and could be used to inform or adjust irrigation schedules accordingly.
4. The uplink messages were logged at one-minute intervals. Although this time interval is adjustable, a one-minute lag was chosen specifically for efficient data collection during the test.
5. This entire procedure was repeated at both test locations.
6. After testing, the uplink messages were downloaded from the gateway in JSON format. This file included detailed information on the status of each message sent by the sensor node and received by the gateway, as well as the corresponding RSSI and SNR values for each transmission. Graphs of SNR and RSSI values of each of the two locations were plotted.

Figure *3.19* and Figure *3.20* show the locations set up at the Farm shelter and CAEC respectively.

Figure 3.19: Setting up the LoRa gateway at the Farm shelter

Figure 3.20: The LoRa gateway set up at CAEC

3.4 Evaluation of the performance of the of the sensor node in enhancing irrigation scheduling

After successfully integrating the sensor node into the existing LoRa-based smart irrigation system and confirming seamless communication within the network, the entire irrigation system was evaluated. This evaluation focused on using real-time data from the sensor node to develop an irrigation schedule that determined both when and how much water should be applied to the field. At the gateway, a Python script was developed using Visual Studio Code to interpret the data received from the sensor node. This script categorized the soil water tension values into three distinct levels of soil moisture, as shown in Table *3.3* below.

Table 3.3: The thresholds followed in categorizing the sensor node uplink messages.

Soil water tension range (kPa)	**Water status**
0 - 9	Wet
10 – 59	Moist
60 - 200	Dry

When the soil moisture level was categorized as wet or moist, no downlink hexadecimal command was sent to the Strega smart valve, and it remained closed. However, once the soil water tension reached or exceeded 60 kPa, indicating dry soil conditions, a downlink hexadecimal message was automatically sent to the Strega smart valve instructing it to open and begin irrigation.

Irrigation continued until the sensor readings showed that the soil water tension had dropped back to 9 kPa, indicating that the soil was sufficiently rehydrated. At this point, the system automatically sends a downlink message to the valve, instructing it to close, and as a result, irrigation is stopped. Figure *3.21* shows the Strega smart valve which automates irrigation in the field based on the hexadecimal downlink messages it receives from the gateway.

Figure 3.21: The Strega smart valve set up in the field.

CHAPTER FOUR: RESULTS AND DISCUSSIONS

4.1 A solar-powered, LoRa-based soil moisture monitoring node.

4.1.1 The sensor node

The first specific objective of this study was to develop a solar-powered, LoRa-based soil moisture monitoring node. This design was developed through the careful integration of various electronic components, each serving a critical role in the system's operation.

The energy supply system is organized into three main stages: energy harvesting, storage, and utilization. It begins with a 15W solar panel that captures solar energy. This energy is regulated by a buck converter to match the required charging voltage for the battery pack. The regulated energy is then stored in a 3S lithium-ion battery pack, which is protected and managed by a 3S Battery Management System (BMS) to ensure safe operation and cell balancing.

From storage, the energy flows to another buck converter, which steps down the battery voltage to a suitable level for the Arduino Uno microcontroller. The Arduino Uno is the central control unit where the electrical energy is ultimately utilized to drive the sensing and communication processes.

To measure the soil moisture tension, a properly calibrated Irrometer 200SS watermark sensor was used in this project and it was connected to the Arduino Uno, which issued the commands for the readings to be captured in real-time.

Since the Arduino Uno outputs signals at 5V and the EBYTE LoRa SX1276 module operates safely at 3.3V logic level, a TXS0108E logic level shifter was placed between them. This ensured bi-directional communication between the two components without risking damage to the LoRa module due to high voltage from the Arduino Uno microcontroller board.

Figure 4.1 shows a fully assembled sensor node that I assembled and deployed at the MUARIK-DABE demonstration farm.

Figure 4.1: A fully assembled sensor node deployed in the field.

4.1.2 Results from the calibration of the watermark sensors

After calibrating the Irrometer 200SS Watermark sensor using the gravimetric method for determining soil moisture content, the resulting data were recorded and are presented in Table *4.1* below.

Table 4.1: Results from calibration of the watermark sensor against the gravimetric method

Watermark sensors (kPa)	**Gravimetric Moisture Content (g/g)**
8.67	34.72
8.88	34.10
9.07	32.81
9.22	30.80
9.33	29.29
9.56	28.12
9.67	27.82
9.89	27.68
9.89	26.76
10.00	26.69
10.00	26.00
10.00	25.89
10.00	25.68
10.00	25.62
11.44	25.26
12.00	25.26
12.67	25.20

The values showed in Table *4.1* above were plotted with gravimetric water content on the Y-axis and soil water potential on the X-axis, resulting in the generation of a calibration curve, as shown in Figure *4.2*.

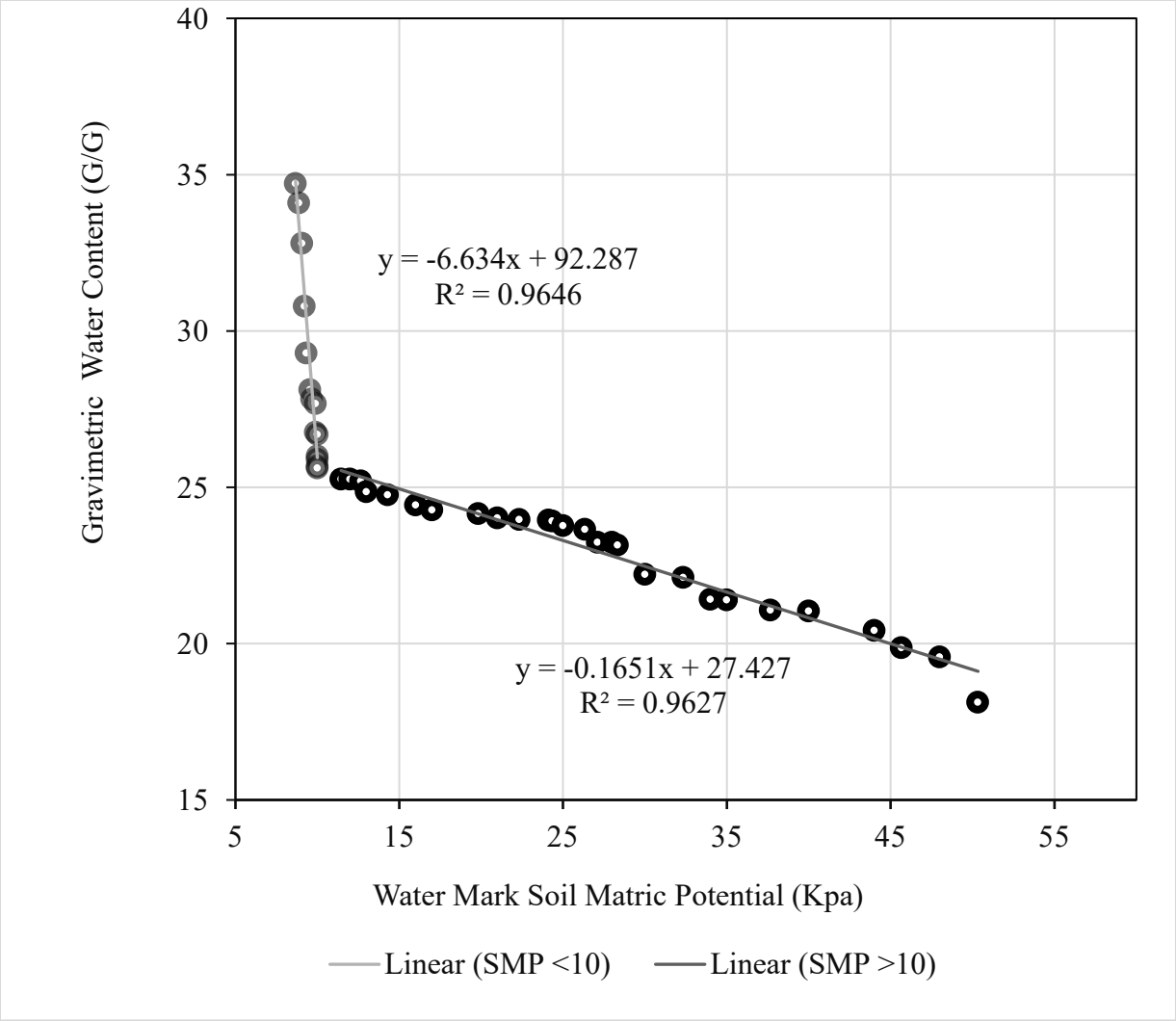

Figure 4.2: Calibration curve of the Irrometer 200SS watermark sensor

This process resulted in the development of a calibration curve comprising two distinct linear equations: one corresponding to soil water potential values less than 10 kPa, and the other for values greater than 10 kPa. Each equation had a very high coefficient of determination (R^2), indicating a strong correlation between the readings obtained using the gravimetric water content of determining soil moisture and the soil water tension values read off from the watermark sensor.

For values less than 10 kPa:

$y = -6.634x + 92.287$, $R^2 = 0.9646$

For values greater than 10 kPa:

$y = -0.1651x + 27.427$, $R^2 = 0.9627$

This calibration equations were integrated into the soil water tension sensing code deployed which was uploaded in to the Arduino Uno microcontroller. Incorporating this equation enabled the system to directly output calibrated soil water tension values based on the raw sensor readings, thereby enhancing the accuracy and reliability of the soil water tension measurements.

4.1.3 Results from the validation of the watermark sensor readings

The soil water tension readings from the watermark sensor and the gravimetric method were recorded and are presented in Table *4.2* below:

Table 4.2: Validation results

Sensor readings(kPa)	Equivalent sensor readings (g/g)	Gravimetric method results(g/g)
30.00	22.474	22.21
32.33	22.089	22.11
34.00	21.814	21.42
35.00	21.649	21.40
37.67	21.208	21.07
40.00	20.823	21.04
44.00	20.163	20.42
45.67	19.887	19.87
48.00	19.502	19.57
50.33	19.118	18.12

The results of the t-test conducted for the validation process using the gravimetric method reveal several key points. The means of the two groups, sensor readings and gravimetric measurements, were 20.950 g/g and 20.723 g/g, respectively. These means are very close, indicating that the sensor's average readings are comparable to those obtained through the gravimetric method.

Examining the variances, we find that the sensor data has a variance of 1.214, while the gravimetric method has a variance of 1.580. These variances are also quite similar, suggesting that the variability in the measurements is consistent between the two methods. The pooled variance, a weighted average of these variances, was calculated to be 1.397.

The degrees of freedom (df) for this test were 18. The calculated t-statistic (t Stat) was 0.429, which shows how much the sample means deviate from each other in units of standard error. The p-value for the two-tailed test (P ($T \leq t$) two-tail) was found to be 0.673. This p-value is much greater than the significance level (alpha) of 0.05, leading us to fail to reject the null hypothesis.

Consequently, this indicates that there is no statistically significant difference between the means of the sensor and gravimetric measurements.

Further supporting this conclusion is the comparison of the absolute value of the t-statistic to the critical value of the t-distribution. The t Stat of 0.429 is far less than the t Critical two-tail value of 2.101, reinforcing the result that the difference between the means is not statistically significant.

Overall, the validation results demonstrate that the sensor readings are consistent and comparable to the traditional gravimetric method, confirming the reliability and accuracy of the watermark sensor for measuring the soil water tension.

4.2 Results from the Programming and Configuration of the Sensor Node for Real-Time Soil Moisture Monitoring and LoRa-Based Communication

The second objective of this study focused on programming and configuring the sensor node to enable accurate real-time soil moisture monitoring and seamless communication with the existing smart LoRa-based irrigation system. To achieve this, Arduino code was developed to initiate communication over the Long-Range Wide Area Network (LoRaWAN). Specifically, this code was written to activate the Ebyte SX1276 LoRa sender module, enabling it to transmit data packets to the LoRa gateway at one-minute intervals. The code incorporated essential joining credentials such as the DEVEUI, APPEUI, and AppKey for successful network registration. On the gateway side, a JavaScript decoder script was implemented within the ChirpStack software platform to interpret the received data. This script converted the transmitted hexadecimal payloads into easily readable soil moisture tension values in kilopascals (kPa), allowing for clear analysis and interpretation.

4.2.1 Received Signal Strength Indicator and Signal to Noise Ratio results

The RSSI and SNR values obtained from the two test sites were recorded in an Excel data sheet, and graphs for each parameter at each location were subsequently plotted for analysis. Figure *4.3* and Figure *4.4* show the RSSI graphs for the values got the farm shelter and CAEC respectively while Figure *4.5* and Figure *4.6* display the corresponding SNR graphs for the same locations.

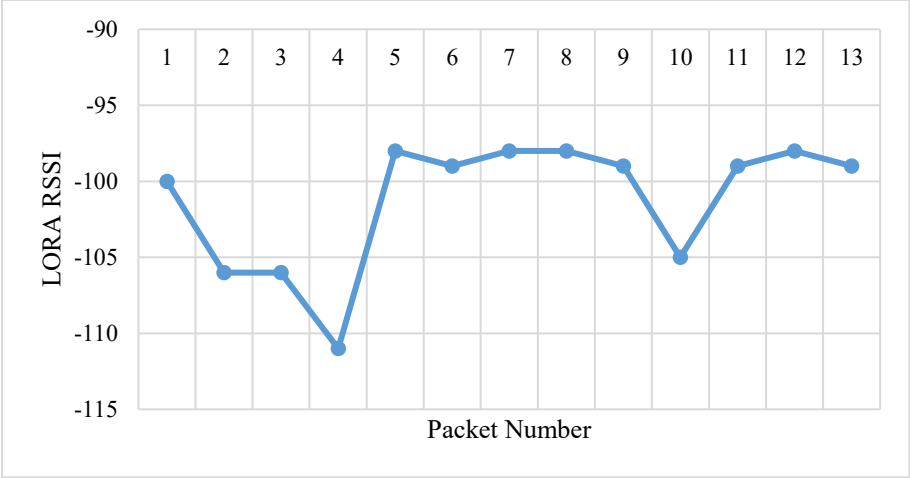

Figure 4.3: A graph showing the RSSI obtained from tests done at the Farm shelter

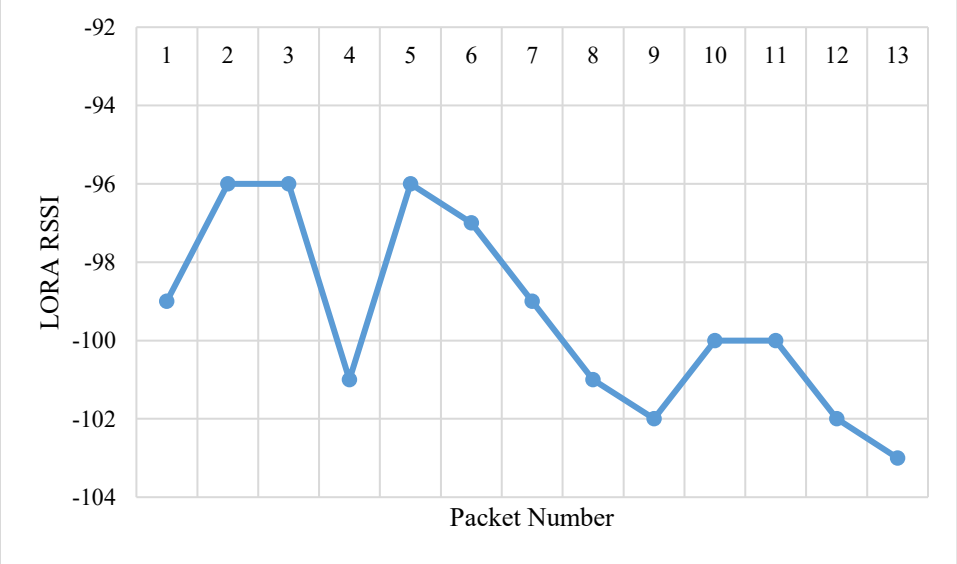

Figure 4.4: A graph showing the RSSI values from tests done at CAEC

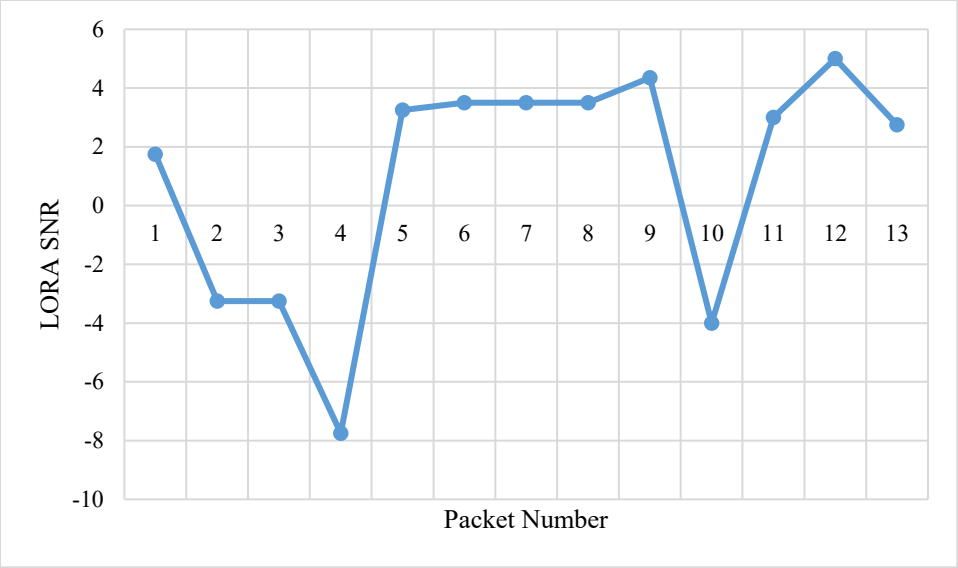

Figure 4.5: A graph showing the SNR values from tests done at the Farm shelter

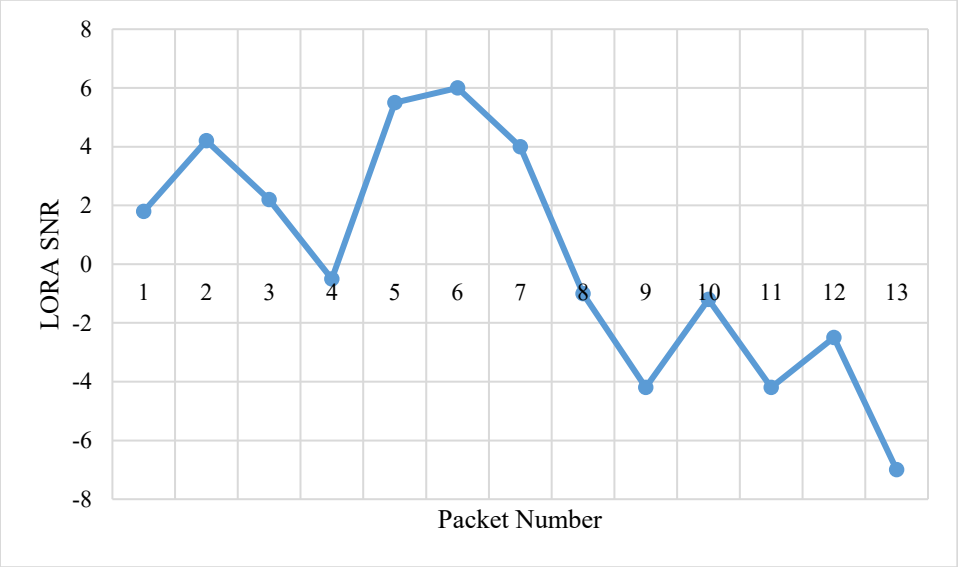

Figure 4.6: A graph showing the SNR values from tests done at CAEC.

4.3 Performance Evaluation of the Sensor Node in Enhancing Irrigation Scheduling

The sensor node effectively transmitted real-time soil water tension data to the LoRa gateway. At the gateway, the Python script accurately categorized the incoming data into three distinct soil moisture levels i.e. wet, moist and dry based on the predefined thresholds in Table *3.3*. This classification allowed the system to assess the exact water requirements of the field.

When the soil water tension reached the dry threshold i.e. ≥60 kPa (17.521 g/g), the system automatically sent a downlink hexadecimal command to the Strega smart valve, instructing it to open and begin irrigation. Field observations confirmed that irrigation was promptly initiated in response to these commands.

As irrigation progressed and the soil moisture level increased, the sensor node detected when soil water tension dropped to 9 kPa (32.581 g/g) or below. In response, the system sent another downlink message to the valve, instructing it to close and thus stopping the irrigation process. This automatic response helped to prevent over-irrigation and ensured that only the required amount of water was applied to the soil.

The entire irrigation cycle starting from detecting dry soil conditions, activating the valve, monitoring soil moisture during irrigation, to automatically shutting off the valve was all executed autonomously. This demonstrated the system's ability to minimize manual intervention while enhancing irrigation scheduling efficiency.

By irrigating only when necessary and stopping once optimal moisture was restored, the system promoted efficient water use and reduced wastage, aligning irrigation directly with actual soil conditions.

Throughout the evaluation period, LoRa communication between the sensor node and the gateway remained stable and reliable. Both uplink and downlink messages were transmitted and received without disruption, enabling uninterrupted system automation. Additionally, the system showed a quick response time, with an average delay of less than one minute between a change in soil condition and the corresponding control action. This matched the configured 1-minute uplink interval, confirming the system's suitability for real-time irrigation control.

4.4 Discussions

A major achievement of this project was the integration of a solar-powered LoRa-based soil moisture monitoring node with Strega smart valves which enabled automated irrigation. The sensor node which was using an Irrometer 200SS Watermark sensor, measured the real-time soil water tension and transmitted the data packets wirelessly to a LoRa gateway. To enable communication, ChirpStack credentials (DEVEUI, APPEUI, AppKey) were programmed into the Arduino code.

At the gateway, a custom JSON decoder (Codec) converted the received hexadecimal uplink data into readable soil moisture values which categorized them as wet, moist, or dry. When dry conditions were detected, the gateway sent a downlink command to open the Strega valve for irrigation. Once moisture was restored to field capacity, a second downlink command was sent to close the valve, completing the automated irrigation cycle.

The evaluation of LoRa signal quality was conducted at two different locations within MUARIK which are the Farm Shelter and the Continuing Agricultural Education Centre (CAEC). The results from the RSSI graphs (Figure *4.3* and Figure *4.4*) reveal a clear difference in signal strength between these two sites.

At the Farm Shelter, higher RSSI values were consistently recorded compared to those at CAEC. The Received Signal Strength Indicator (RSSI) is a measure of the power level received by the gateway from the sensor node, expressed in decibels (dBm). A higher RSSI indicates a stronger and more reliable signal, which enhances communication performance. Conversely, low RSSI values suggest weak signal strength, increasing the likelihood of data loss or communication errors. The high RSSI values at the Farm Shelter can be attributed to the clear line of sight between the sensor node and the gateway, with minimal obstructions such as buildings or trees. This unobstructed path allowed for efficient signal transmission and reduced the risk of packet loss. Notably, when the gateway was installed at the Farm Shelter, the sensor node established connection almost instantly.

In contrast, when the gateway was placed at CAEC, the recorded RSSI values were significantly lower. This location had numerous physical obstructions such trees and buildings which interfered with the signal transmission. As a result, signal strength reduced, some data packets were lost, and the connection between the sensor node and the gateway was delayed by approximately five minutes. These factors contributed to the reduced communication reliability observed at CAEC.

Similarly, the Signal-to-Noise Ratio (SNR) analysis (Figure *4.5* and Figure *4.6*) supports these findings. The Farm Shelter recorded higher SNR values compared to CAEC. SNR is the ratio between the power of the desired signal and the background noise, also expressed in decibels (dB). A higher SNR reflects a clearer signal with less interference, resulting in more accurate data transmission. Conversely, a lower SNR indicates that background noise is relatively strong, which can degrade communication quality.

At the Farm Shelter, higher SNR values were observed due to the low levels of environmental noise and interference. In contrast, CAEC recorded lower SNR values, likely caused by multiple noise sources such as moving vehicles, wind, and other disturbances. These environmental factors degraded the signal clarity, contributing to less reliable communication.

CHAPTER FIVE: CONCLUSIONS AND RECOMMENDATIONS

5.1 Conclusions

This project successfully demonstrated the feasibility and effectiveness of a solar-powered, LoRa-based soil moisture monitoring sensor node for enhancing smart irrigation scheduling. The developed system enabled the seamless real-time data transmission between the sensor node and the LoRa gateway, which in turn eased automated irrigation decisions based on accurate soil moisture readings.

The findings from this study highlight the critical importance of gateway placement in achieving reliable system performance. In order to achieve reliable results, the gateway should be positioned with a clear line of sight to the sensor node. This conclusion is supported by signal strength comparisons conducted at two test locations: CAEC and the Farmer's Shelter. The signals recorded at the Farmer's Shelter, where there were minimal obstructions, were significantly more stable and reliable than those from CAEC, where buildings and trees interfered with the wireless communication.

Stronger and more consistent signals ensured faster and more accurate transmission of soil moisture data, which greatly facilitated the automation of irrigation. With reliable communication, the system was able to efficiently trigger the Strega smart valves, sending timely commands on when to open or close based on the real-time soil moisture status. This ultimately improved the water use efficiency and reduced manual intervention.

5.2 Recommendations

Based on the findings of this project, I came up with the several recommendations some of which are explained below. All these had a major purpose of enhancing the performance, scalability, and applicability of the developed LoRa-based soil moisture monitoring and irrigation scheduling system.

Firstly, the irrigator should ensure the optimal placement of the LoRa gateway. Given the layout of most farms in Uganda, achieving a clear line of sight may be challenging. To address this, access roads can be created to improve visibility and reduce signal interference. The gateway should be

installed in locations with minimal obstructions and a clear line of sight to the sensor nodes to ensure strong and stable signal reception.

Secondly, when installing the gateway's antenna, it should be positioned at the highest possible elevation, such as on the roof of a house. This elevation helps improve signal reception from the sensor nodes. Mounting the antenna on elevated structures or poles can significantly reduce signal interference, thereby enhancing RSSI and SNR values.

In order to improve on the spatial coverage and measurement accuracy, additional soil moisture sensor nodes should be deployed across different sections of the field. To accommodate more Watermark sensors, microcontroller boards with a higher number of input/output pins i.e. the Arduino Due or Arduino Mega, should be used instead of the Arduino Uno. Furthermore, integrating additional environmental sensors such as temperature, humidity, and rainfall sensors would provide a more complete understanding of field conditions and support more intelligent, data-driven irrigation decisions.

In conclusion, the system should be tested over a full growing season to enable it to record the amount of water used to irrigate a specific crop throughout that period.

REFERENCES

Ahmed, S. I., Minjuan, W., Yanzhao, R., Qinglan, S., Hammad, M. M., Sha, T., Qiang, C., & Wanlin, G. (2019). Performance analysis of dielectric soil moisture sensor. *Soil and Water Research*, *14*(4), 195–199. https://doi.org/10.17221/74/2018-SWR

Bamwesigye, D., Doli, A., Adamu, K. J., & Mansaray, S. K. (2020). *A Review of the Political Economy of Agriculture in Uganda : Women , Property Rights , and Other Challenges*. *8*(1), 1–10. https://doi.org/10.13189/ujar.2020.080101

Bezerra, N. S., Åhlund, C., Saguna, S., & de Sousa, V. A. (2019). Temperature impact in LoraWAN—A case study in northern Sweden. *Sensors (Switzerland)*, *19*(20), 1–30. https://doi.org/10.3390/s19204414

Bond, W. J., & Hutchinson, P. a. (2006). *Principles , Implementation , Installation and Operation of the Tube Tensiometer Drainage Meter*. *June*.

Bor, M., Vidler, J., & Roedig, U. (2016). Lora for the internet of things. *International Conference on Embedded Wireless Systems and Networks*, 361–366.

Chard, J. (2002). Watermark Soil Moisture Sensors: Characteristics and Operating Instructions. *Utah State University*, 1–8. http://usu.edu/cpl/PDF/WatermarkOperatingInstructions2.pdf

Darko, R. O., Shouqi, Y., Junping, L., Haofang, Y., & Xingye, Z. (2017). *Overview of advances in improving uniformity and water use efficiency of sprinkler irrigation*. *10*(2), 1–15. https://doi.org/10.3965/j.ijabe.20171002.1817

Datta, S., Taghvaeian, S., Ochsner, T. E., Moriasi, D., Gowda, P., & Steiner, J. L. (2018). *Performance Assessment of Five Different Soil Moisture Sensors under Irrigated Field Conditions in Oklahoma*. 1–17. https://doi.org/10.3390/s18113786

Devalal, S., & Karthikeyan, A. (2018). LoRa Technology - An Overview. *Proceedings of the 2nd International Conference on Electronics, Communication and Aerospace Technology, ICECA 2018*, *Iceca 2018*, 284–290. https://doi.org/10.1109/ICECA.2018.8474715

Garc, L., Parra, L., Jimenez, J. M., & Lloret, J. (2020). *IoT-Based Smart Irrigation Systems : An Overview on the Recent Trends on Sensors and IoT Systems for Irrigation in Precision Agriculture*.

Garg, A., Munoth, P., & Goyal, R. (2016). Application of Soil Moisture Sensors in Agriculture: a Review. *Proceedings of International Conference on Hydraulic* , *December*, 8–10. https://www.researchgate.net/publication/311607215

Goap, A., Sharma, D., Shukla, A. K., & Krishna, C. R. (2018). *An IoT based smart irrigation management system using Machine learning and open source technologies*. *155*(May), 41–49.

Gu, Z., Ph, D., Qi, Z., Burghate, R., Yuan, S., Jiao, X., Xu, J., & Asce, A. M. (2020). *Irrigation Scheduling Approaches and Applications : A Review*. *146*(6). https://doi.org/10.1061/(ASCE)IR.1943-4774.0001464

Haxhibeqiri, J., De Poorter, E., Moerman, I., & Hoebeke, J. (2018). A survey of LoRaWAN for IoT: From technology to application. *Sensors (Switzerland)*, *18*(11). https://doi.org/10.3390/s18113995

Ismailov, A. S. (2022). *Study of arduino microcontroller board*. *3*(3), 172–179.

Jara-Rojas, R., Engler, A., Adasme-Berríos, C., Carrasco-Benavides, M., Ortega-Farias, S., & Mediavilla, W. (2018). Adoption of irrigation scheduling: Role of extension and training in central Chile. *Environmental Engineering and Management Journal*, *17*(12), 2873–2880. https://doi.org/10.30638/eemj.2018.287

Jarwar, A. H., Wang, X., Wang, L., Zhanshuai, L., Zhaoyang, Q., Mangi, N., Pengjia, B., Ma, Q., & Shuli, F. (2019). *Performance and evaluation of drip irrigation system , and its future advantages*. *4*(1).

Jones, H. G. (2004). *Irrigation scheduling : advantages and pitfalls of plant-based methods*. *55*(407), 2427–2436. https://doi.org/10.1093/jxb/erh213

Koech, R., & Langat, P. (2018). Improving irrigation water use efficiency: A review of advances, challenges and opportunities in the Australian context. *Water (Switzerland)*, *10*(12). https://doi.org/10.3390/w10121771

Light, J., Mitchell, A., Barnum, J., & Shock, C. (2004). Granular Matrix Sensors for Irrigation Management. *Chemistry & …*. http://onlinelibrary.wiley.com/doi/10.1002/cbdv.200490137/abstract

No Title. (2024). https://www.irrometer.com/200ss.html

Obaideen, K., Yousef, B. A. A., AlMallahi, M. N., Tan, Y. C., Mahmoud, M., Jaber, H., & Ramadan, M. (2022). An overview of smart irrigation systems using IoT. *Energy Nexus*, *7*(July), 100124. https://doi.org/10.1016/j.nexus.2022.100124

Okiror, P., Lejju, J. B., Bahati, J., Rugunda, G. K., Sebuuwufu, C. I., Mulindwa, P., & Ocan, J. J. (2017). *Suitability of Kabanyolo Soils for Fruit and Vegetable Production*. 19–33. https://doi.org/10.4236/ojss.2017.72002

Orouskhani, E., Sahoo, S., Agyeman, B., Bo, S., & Liu, J. (2023). Impact of sensor placement in soil water estimation: a real-case study. *Irrigation Science*, *41*(3), 395–411. https://doi.org/10.1007/s00271-023-00845-y

Pradesh, U. (2018). *A Review on Types of Irrigation System and their Advantages*. *5*(3), 79–84.

Quy, V. K., Hau, N. Van, Anh, D. Van, Quy, N. M., & Ban, N. T. (2022). *applied sciences IoT-Enabled Smart Agriculture : Architecture , Applications , and Challenges*.

Rasheed, M. W., Tang, J., Sarwar, A., Shah, S., Saddique, N., Khan, M. U., Khan, M. I., Nawaz, S., Shamshiri, R. R., Aziz, M., & Sultan, M. (2022). *Soil Moisture Measuring Techniques and Factors Affecting the Moisture Dynamics : A Comprehensive Review*.

Sarkar, N., Chandra, B., Viswavidyalaya, K., & Majhi, T. (2019). Study on soil moisture variations in responding to Tensiometer and soil moisture meter with respect to gravimetric method. *International Journal of Chemical Studies*, *7*(4), 3179–3188. https://www.researchgate.net/publication/335890411

Sciences, O. (2024). *An Internet of Things (IoT)-based smart irrigation and crop suggestion platform for enhanced precision agriculture Kartik Ingole * Dinesh Padole*. *45*(4), 873–883.

Shafi, U., Mumtaz, R., García-Nieto, J., Hassan, S. A., Zaidi, S. A. R., & Iqbal, N. (2019). Precision agriculture techniques and practices: From considerations to applications. *Sensors (Switzerland)*, *19*(17), 1–25. https://doi.org/10.3390/s19173796

Sharma, P. K., Kumar, D., Srivastava, H. S., & Patel, P. (2018). Assessment of Different Methods for Soil Moisture Estimation : A Review. *Journal of Remote Sensing & GIS*, *9*(1), 57–73.

Shock, C. C., & Wang, F. (2010). *Soil Water Tension , a Powerful Measurement for Productivity*

and Stewardship. 178–185.

Shock, C. C., Wang, F. X., Flock, R., & Feibert, E. (2013). *Irrigation Monitoring Using Soil Water Tension*. *March*.

Smolau, S. (2009). *Evaluation of the Received Signal Strength Indicator for Node Localization in Wireless Sensor Networks*.

Stacheder, M., Koeniger, F., & Schuhmann, R. (2009). New Dielectric Sensors and Sensing Techniques for Soil and Snow Moisture Measurements. *Sensors*, *9*(4), 2951–2967. https://doi.org/10.3390/s90402951

Sui, R. (2018). *Irrigation Scheduling Using Soil Moisture Sensors*. *10*(1), 1–11. https://doi.org/10.5539/jas.v10n1p1

Tantalaki, N., Souravlas, S., & Roumeliotis, M. (2019). Data-Driven Decision Making in Precision Agriculture: The Rise of Big Data in Agricultural Systems. *Journal of Agricultural and Food Information*, *20*(4), 344–380. https://doi.org/10.1080/10496505.2019.1638264

Ting, Y. T., & Chan, K. Y. (2024a). Optimising performances of LoRa based IoT enabled wireless sensor network for smart agriculture. *Journal of Agriculture and Food Research*, *16*(February), 101093. https://doi.org/10.1016/j.jafr.2024.101093

Ting, Y. T., & Chan, K. Y. (2024b). Optimising performances of LoRa based IoT enabled wireless sensor network for smart agriculture. *Journal of Agriculture and Food Research*, *16*(September 2023), 101093. https://doi.org/10.1016/j.jafr.2024.101093

UBOS. (2022). *Press Release Consumer Price Indices and Inflation Rates*. www.ubos.org

United Nations (UN). (2024). World Population Prospects 2024. In *United Nation* (Issue 9). www.un.org/development/ desa/pd/.

Vallejo-g, D., Osorio, M., & Hincapi, C. A. (2023). *Smart Irrigation Systems in Agriculture : A Systematic Review*. 1–25.

Velmurugan, S., Balaji, V., Bharathi, T. M., & Saravanan, K. (2020). *An IOT based Smart Irrigation System using Soil Moisture and Weather Prediction*. *8*(07), 1–4.

Vera, J., Conejero, W., Mira-García, A. B., Conesa, M. R., & Ruiz-Sánchez, M. C. (2021). Towards irrigation automation based on dielectric soil sensors. *Journal of Horticultural*

Science and Biotechnology, *96*(6), 696–707. https://doi.org/10.1080/14620316.2021.1906761

Vories, E., & Sudduth, K. (2021). Determining sensor-based field capacity for irrigation scheduling. *Agricultural Water Management*, *250*(September 2020), 106860. https://doi.org/10.1016/j.agwat.2021.106860

Wanyama, J., Ssegane, H., Kisekka, I., Komakech, A. J., Banadda, N., Zziwa, A., Ebong, T. O., Mutumba, C., Kiggundu, N., Kayizi, R. K., Mucunguzi, D. B., & Kiyimba, F. L. (2017). Irrigation Development in Uganda: Constraints, Lessons Learned, and Future Perspectives. *Journal of Irrigation and Drainage Engineering*, *143*(5). https://doi.org/10.1061/(asce)ir.1943-4774.0001159

Yu, L., Gao, W., Shamshiri, R. R., Tao, S., Ren, Y., Zhang, Y., & Su, G. (2021). Review of research progress on soil moisture sensor technology. *International Journal of Agricultural and Biological Engineering*, *14*(4), 32–42. https://doi.org/10.25165/j.ijabe.20211404.6404